Geo-Spatial Approach for Urban Green Space and Environmental Quality Assessment: a case study of Addis Ababa, Ethiopia

Ayda Meskere Tilaye

A Thesis Submitted to the Department of Geomatics Engineering
School of Civil Engineering and Architecture

Presented in Partial Fulfillment of the Requirement for the Degree of Master's in Geo-Informatics

Office of Graduate Studies

Adama Science and Technology University

October, 2024
Adama, Ethiopia

Geo-Spatial Approach for Urban Green Space and Environmental Quality Assessment: a case study of Addis Ababa, Ethiopia

Ayda Meskere Tilaye

Advisor
Getachew Brhanemeskel (PhD)

A Thesis Submitted to the Department of Geomatics Engineering
School of Civil Engineering and Architecture

Presented in Partial Fulfillment of the Requirement for the Degree of Master's in Geo-Informatics

October, 2024
Adama, Ethiopia

Approval Sheet

I the advisors of the thesis entitled "Geo-Spatial Approach for Urban Green Space and Environmental Quality Assessment: a case study of Addis Ababa, Ethiopia" and developed by Ayda Meskere, here by certify that the recommendation and suggestions made by the board of examiners are appropriately incorporated into the final version of the thesis.

Getachew Brhanemeskel (PhD)
______________________ ______________________ ______________________
Major Advisor/Supervisor Signature Date

We, the undersigned, members of the Board of Examiners of the thesis by Ayda Meskere have read and evaluated the thesis entitled "Geo-Spatial Approach for Urban Green Space and Environmental Quality Assessment: a case study of Addis Ababa, Ethiopia" and examined the candidate during open defense. This is, therefore, to certify that the thesis is accepted for partial fulfillment of the requirement of the degree of Master of Science in Geo-informatics.

Yared Girma (PhD)
______________________ ______________________ ______________________
Chairperson Signature Date

Roba Gemechu (PhD)
______________________ ______________________ ______________________
Internal Examiner Signature Date

Sitotaw Haile (PhD)
______________________ ______________________ ______________________
External Examiner Signature Date

Final approval and acceptance of the thesis is contingent upon submission of its final copy to the Office of Postgraduate Studies (OPGS) through the Department Graduate Council (DGC) and School Graduate Committee (SGC).

______________________ ______________________ ______________________
Department Head Signature Date

______________________ ______________________ ______________________
School Dean Signature Date

______________________ ______________________ ______________________
Office of Postgraduate Studies, Dean Signature Date

Declaration

I hereby declare that this Master Thesis entitled "Geo-Spatial Approach for Urban Green Space and Environmental Quality Assessment: a case study of Addis Ababa, Ethiopia" is my original work. That is, it has not been submitted for the award of any academic degree, diploma or certificate in any other university. All sources of materials that are used for this thesis have been duly acknowledged through citation.

Ayda Meskere Tilaye

Name of student	Signature	Date

Recommendation

I, the advisor of this thesis, hereby certify that I have read the revised version of the thesis entitled "Geo-Spatial Approach for Urban Green Space and Environmental Quality Assessment: a case study of Addis Ababa, Ethiopia" prepared under my guidance by Ayda Meskere. Therefore, I recommend the submission of revised version of the thesis to the department following the applicable procedures.

Getachew Brhanemeskel (PhD)

______________________	______________________	______________
Major Advisor/Supervisor	Signature	Date

Acknowledgment

Firstly, I extend my deepest gratitude to Almighty God, the Lord of all, for granting me health and making all things possible throughout my life. His blessings and guidance have been my constant support. I am immensely thankful to my advisor, Dr. Getachew Brhanemeskel. His unwavering guidance, supervision, and insightful feedback have been invaluable throughout the completion of this thesis. His expertise and dedication have inspired and motivated me to strive for excellence. I also wish to express my appreciation to the staff at the Ethiopian National Meteorology Agency. Their cooperation and assistance in providing all the essential data and information about the study area were crucial for my research. A special thanks goes to the Space Science and Geospatial Institute for their prompt provision of study area boundary. Their support greatly facilitated the progress of my work. I must also acknowledge the encouragement and support from my parents, whose faith in me has been a constant source of strength. Their love and sacrifices have always driven me to pursue my goals. To my friends and course instructors, your constant encouragement, understanding, and advice have been invaluable. Your support has sustained me through the challenges of this journey, and for that, I am profoundly grateful. Lastly, I am grateful to everyone who contributed, directly or indirectly, to the successful completion of this thesis. Your help and encouragement have made this accomplishment possible. Thank you all.

Table of Contents

List of tables

List of figures

List of Acronyms

AEPA	Addis Ababa Environmental Protection Authority
CR	Consistency Ratio
ERDAS	Earth Resources Data Analysis System
ESS	Ethiopia Statistical Service
ETM+	Enhancement Thematic Mapper Plus
GIS	Geographic Information System
GPS	Global Positioning System
GSA	Geospatial Approach
LULC	Land-use and Land-cover
MCE	Multi-criteria Evaluation
NDBI	Normalized Difference Built-up Index
NDVI	Normalized Deference Vegetation Index
NMI	National Meteorological Institute
OLI	Operational Land Imager
POS	Parks and Open spaces
SSGI	Space Science and Geospatial Institute
TIRS	Thermal Infrared Sensor
TM	Thematic Mapper
UEQ	Urban Environmental Quality
UGS	Urban Green Space

Abstract

The degradation of environmental conditions due to unsustainable human activities has made cities increasingly stressful. This unsustainable use of the urban environment has led to a decline in various environmental aspects, including natural vegetation, climate, wetlands, and wildlife. The rapid expansion of infrastructure and population growth has significantly altered the natural, cultural, and social structures of cities. Regular updates on Urban Environmental Quality (UEQ) are crucial for effective city planning. The aim of the study was to explore the use of urban greenery as an indicator of changes in Urban Environmental Quality (UEQ) in Addis Ababa, using natural parameters from satellite imagery and socioeconomic data from census records. The study employed a quantitative approach, integrating physical environmental variables such as land-use/land-cover (LULC), land surface temperature (LST), normalized difference vegetation index (NDVI), and socioeconomic indicators, including population density and greenhouse gas emissions. Data were drawn from Landsat imagery for the years 1993, 2003, 2014, and 2024. These datasets were analyzed through regression analysis, factor analysis, and weight overlay analysis, leading to the identification of key factors affecting environmental quality: greenness, crowdedness, heat island effect, and greenhouse gas emissions. A risk map was subsequently developed to reflect varying environmental quality across sub-cities. The results of the study indicate a decline in Addis Ababa's environmental quality, with Addis Ketema sub-city at very high to high risk, Arada and Kirkos at high to moderate risk, and Bole, Lideta, Kolfe, Nifas Silk Lafto, and Lemi Kura at moderate to low risk. Gulele and Yeka sub-cities exhibited the lowest risk levels. The study recommended that future studies incorporate additional parameters to provide a comprehensive understanding of changes in the city's greenness and to address the adverse effects of development activities, such as the increase in population density and the reduction of green spaces.

Keywords: Urban Environmental Quality, Urban Greenery Space.

CHAPTER I: INTRODUCTION

1.1. Background of the Study

The quality of the urban environment is progressively declining as major cities, particularly those of considerable size, are reaching saturation points and struggling to manage the growing strain on their infrastructure, incorporating green spaces into urban planning is crucial for achieving sustainable environmental quality. Nevertheless, the concept of urban environmental quality is intricate, influenced by both human and natural factors operating across various spatial scales (Asadi et al., 2007). The assessment of urban environmental quality involves a planning process that places significance on social, economic, cultural, physical, and emotional indicators, encompassing both tangible and intangible aspects (Opeye et al., 2014). Environmental planners have evaluated urban areas, recognizing the significant contribution of urban green spaces and vegetation cover in maintaining a harmonious connection between humans and the environment. These green spaces, constituting fundamental urban infrastructure, provide substantial aesthetic and ecological benefits to the city. They also contribute to community pride, public health, and overall quality of life (Low et al., 2007).

Urban greenery refers to the comprehensive coverage of outdoor areas adorned with trees, shrubs, ornamental plants, or grass. Instances of these areas include squares, parks, tree-lined streets, groves, and cultivated spaces within the premises of public or private structures such as schools and residential complexes (Aravadinou & Evmorphopoulou, 1999). Parks and open spaces (POS) contribute to a heightened variety of green environments, exerting significant influences on environmental quality in numerous major cities globally (Jim & Chen, 2006).

The presence of green spaces within a contemporary urban setting is anticipated to enhance air quality, diminish noise and air pollution, and improve the aesthetic appeal of the environment. The incorporation of urban greenery holds significant importance in overall city planning, as its advantages directly influence both the environment and the residents' quality of life. Urban green spaces serve as an indicator of the environmental quality of an urban area (Faryadi & Taheri, 2008). However, due to its complex, multifaceted, and interdisciplinary nature, relying on a single indicator is insufficient for assessing environmental quality (Chiesura, 2004).

A comprehensive evaluation necessitates the integration of various elements. Crucial variables for gauging urban environmental quality include urban greenery, built-up areas, carbon emissions, temperature, humidity, waste disposal, accessibility to major roads, and population density. These variables collectively play a substantial role in influencing environmental quality. A significant challenge in ensuring urban environmental quality lies in the complexity of modeling and predicting the interactions among the various aspects and variables associated with it (Liang & Weng, 2011). In this study, the focus is on identifying a suitable distribution of urban green spaces and vegetation density as primary indicators for enhancing air quality, thereby contributing to overall improvements in urban environmental conditions. Factors such as building density, population density, temperature, humidity, waste disposal practices, proximity to major roads, and carbon emissions are recognized as key indicators of urban environmental degradation. Understanding the underlying causal factors is essential for evaluating and sustaining a healthy urban environment (Donovan & Butry, 2010).

The assessment of environmental degradation necessitates an effective geospatial approach, considering the geographical location of features on the Earth's surface. This method is crucial as it reveals how outcomes vary when the spatial locations of analyzed phenomena change (Seto et al., 2012). Given the diverse range of numerical methods within the realm of geospatial approaches, these techniques play a vital role in comprehending and addressing urban environmental challenges (Cromley, 2013).

Green spaces provide significant health benefits by promoting physical activity and enhancing mental well-being. According to the World Health Organization (WHO), access to urban green spaces is linked to reduced obesity rates and lower incidences of mental health disorders, such as anxiety and depression (WHO, 2016). Research has shown that living near green areas can decrease all-cause mortality rates by up to 12% (Holt et al., 2021). Moreover, green spaces improve cognitive functions in children and contribute to emotional stability, as interactions with nature have been associated with lower levels of anger, fear, and sadness (Faber Taylor & Kuo, 2009; Kaplan & Kaplan, 1989).

Beyond health, green spaces play a crucial role in climate regulation and enhancing urban aesthetics. They mitigate the urban heat island effect by providing shade and improving air quality through pollutant filtration, benefiting respiratory health (EPA, 2014). Additionally, green spaces foster community cohesion by serving as social hubs, enhancing neighborhood safety and life satisfaction (Kuo, 2003). They also support biodiversity, providing essential habitats for various species and promoting ecosystem services, as emphasized by the Convention on Biological Diversity (CBD, 2020). These multifaceted benefits underscore the importance of integrating green spaces into urban planning for healthier, more sustainable communities.

Geospatial technology, encompassing tools like Geographic Information Systems (GIS), remote sensing, and global positioning systems (GPS), plays a crucial role in assessing environmental quality globally, including in Africa and Ethiopia. By enabling the collection, analysis, and visualization of spatial data, these technologies facilitate a better understanding of environmental conditions and trends. For instance, GIS allows researchers and policymakers to map and analyze various environmental factors, such as land use, vegetation cover, and pollution levels, thereby providing insights that inform sustainable management practices (Kumar & Kumar, 2020). Remote sensing technologies, such as satellite imagery, offer real-time data on changes in land cover and land use, enabling assessments of environmental degradation and climate change impacts (Turner et al., 2015).

In Africa, geospatial technologies are increasingly being applied to address pressing environmental issues, such as deforestation, desertification, and water resource management. For example, studies have shown that remote sensing is instrumental in monitoring deforestation rates in countries like Kenya and Tanzania, aiding in conservation efforts (Hansen et al., 2013). In Ethiopia, geospatial tools have been pivotal in evaluating land degradation and environmental quality, particularly in the context of rapid urbanization and agricultural expansion. Research has demonstrated the effectiveness of GIS in analyzing soil erosion and assessing the health of ecosystems, ultimately contributing to better land management and conservation strategies (Ayele & Tesfaye, 2021). As such, the integration of geospatial technologies into environmental assessments not only enhances data accuracy but also supports informed decision-making, thereby promoting sustainable development across various regions.

With this hypothesis as a foundation, the primary objective of the study is to evaluate the environmental conditions of Addis Ababa by considering both natural and social parameters. The research aims to target key areas of concern through the application of GIS and remote sensing techniques.

1.2. Statement of the Problem

The swift expansion of urban areas gives rise to numerous challenges, as it exerts significant pressures on land, water, housing, transportation, healthcare, and education. The economic, cultural, and social fabric of cities, as well as their natural landscapes, undergoes continuous transformation, influenced by the rapid progress in science and technology. Unfortunately, the substantial growth in urban populations often occurs without adequate development planning. Consequently, cities experience heightened stress levels due to unfavorable environmental conditions resulting from unsustainable human impacts on the environment.

The lack of sustainable utilization of the urban environment compromises its overall quality, leading to the deterioration of various environmental factors, including natural vegetation, climate, wetlands, and wildlife, among others. There is an increasing need to develop a method for identifying changes in the urban environment. Indicators are essential for characterizing and simplifying complex phenomena, thereby enhancing our understanding of intricate realities. Typically, these indicators offer valuable insights into the dynamics occurring within a system. They often involve the quantification and aggregation of measurable and monitor able data, facilitating the evaluation of whether changes are indeed taking place. Given the complexity of the urban environment as a system, the measurement of changes in urban environmental quality is achievable primarily through the use of indicators.

Addis Ababa faces a critical shortage of urban green spaces, with approximately 1,200 hectares designated for this purpose, accounting for only about 8% of the city's total area (Addis Ababa City Administration, 2022). This figure falls significantly below the World Health Organization's (WHO) recommendation of 9 square meters of green space per resident for urban environments. With a population nearing 5 million people, the demand for accessible green areas is immense (Ethiopian Statistical Service, 2022).

The uneven distribution of green spaces exacerbates the problem, as evidenced by disparities among the city's sub-cities. For instance, neighborhoods such as Addis Ketema and Arada have less than 1 hectare of public parkland per 1,000 residents, while areas like Bole enjoy more extensive green areas. This inequity in access to green spaces poses serious health risks; studies indicate that residents in areas with limited green environments report higher instances of mental health issues, respiratory diseases, and obesity-related problems (Ethiopian Public Health Institute, 2021). A recent health survey conducted by the city's health bureau revealed that approximately 30% of respondents living in green space-deficient areas experience chronic stress, compared to only 15% in neighborhoods with sufficient access to green areas.

Given these challenges, addressing the inadequacy of urban green spaces in Addis Ababa is crucial for enhancing both environmental quality and the overall health and well-being of its residents.

This paper primarily focused on the extraction of greenness. The assessment involved analyzing land-use/land-cover changes, determining the appropriate distribution of urban green spaces, and gauging vegetation density using NDVI. Urban heat island effects, carbon emissions, building density, and population density were considered as initial indicators to investigate changes in urban environmental quality within the study area.

While numerous studies have examined environmental quality and urban green spaces, their methodologies and results vary significantly. Some research utilized outdated data and software for these evaluations. Furthermore, administrative boundaries have evolved: Addis Ababa's area was previously measured at 527 km² with 10 sub-cities, but it now covers 430 km² and includes 11 sub-cities. Land use and land cover have also undergone dynamic changes. This situation underscores the need for a more accurate understanding of the factors affecting urban green spaces and their impact on environmental quality. Therefore, this study aims to address these gaps by employing a range of modern geospatial software tools.

1.3. Objective of the Problem

1.3.1. General Objective

The general objective of this research was to assess the environmental quality of the eleven sub-cities within Addis Ababa by utilizing both natural and social parameters. These parameters were derived from remote sensing satellite imagery and supplementary secondary data.

1.3.2. Specific Objective

To accomplish the general objective, four specific objectives were developed.
These include:

- To evaluate the shifting trends in environmental quality in Addis Ababa city by analyzing land use and land cover patterns;
- To determine the proportion of urban greenery in the study area using NDVI;
- To assess the urban environment through both qualitative and quantitative means using the weighted overlay method;
- To create various thematic maps of the study area that assesses environmental quality.

1.4. Research Questions

Understanding assessment of Urban Green Space and Environmental Quality All actions aligned with the stated general and specific objectives should be consistent with the following research question.

I. What are the spatiotemporal patterns of LU/LC changes of the study area?

II. What is the percentage of urban green space in the study area?

III. What is the impact of LU/LC dynamics on urban environment change in the study area?

IV. How does the distribution of urban green spaces influence environmental quality in the study area?

1.5. Scope of the Study

The study focused specifically on the eleven sub-cities of Addis Ababa. Throughout the research, thematic maps were created to illustrate key elements, including urban greenery, greenhouse gas emissions, population density, building density, urban thermal heat, and land use/land cover. Ultimately, these analyses culminated in the development of an environmental quality map. Every effort was made to conduct the study in a systematic and logical manner.

1.6. Significance of the Study

In an ever-changing world, prioritizing the well-being of urban environments is crucial as environmental factors continually evolve. This study aims to support environmental planners and policymakers in enhancing the quality of urban areas by promoting the establishment of green spaces in polluted regions. The findings offer valuable insights for various stakeholders, including community members, policymakers, and environmental organizations, enabling informed decision-making and effective resource allocation.

Additionally, this research serves as a foundational dataset for future studies, fostering ongoing investigations into urban environmental quality and the impact of green space initiatives. By utilizing these results, stakeholders can collaboratively develop strategies to create healthier and more sustainable urban environments for all.

This study employs specific operational definitions to clarify key concepts related to urban green spaces and environmental quality in Addis Ababa. Urban green space is defined as public parks and vegetated areas within the city that cover at least 0.1 hectares, contributing to community recreation, biodiversity, and environmental health. Environmental quality is assessed through indicators such as air quality (measured by particulate matter and carbon dioxide levels.

Additionally, greenhouse gas emissions are quantified in metric tons per year, accounting for gases like carbon dioxide and methane released from urban activities. Population density and building density are measured by the number of residents and total floor area of buildings per square kilometer, respectively, providing insight into urban development and its impact on green space accessibility.

1.7. Limitations of the study

The temperature and rainfall data obtained from the National Meteorological Agency included some missing or null daily records. These gaps may have influenced the accuracy of the findings related to atmospheric temperature.

1.8. Thesis Paper Organizations

This thesis was organized into five chapters, each with a specific focus. It began with an introductory chapter that covered the background, problem statement, study objectives, research questions, scope, significance, and limitations. The next chapter then explored the relevant literature reviews. The third chapter detailed the study area, the data and software employed, the methodologies used, and various analyses, including land-use/land-cover change detection, calculation of the Normalized Difference Vegetation Index, extraction of urban green spaces, Land Surface Temperature analysis, population density assessment, built-up density evaluation, air quality analysis, and spatial interpolation techniques. The fourth chapter provided the results and discussions based on the comprehensive analysis of the thesis. The final chapter then concluded with a summary of the thesis, including its conclusions and recommendations.

CHAPTER II: LITRATURE REVIEW

2.1. Theory Related to Urban Green Space and Environmental Quality

Urban green spaces, including parks, gardens, and natural landscapes within cities, play a crucial role in enhancing environmental quality and the overall well-being of urban residents. These spaces offer essential ecosystem services such as air purification, water filtration, temperature regulation, and noise reduction, which collectively contribute to public health by mitigating pollution and respiratory issues (Bolund & Hunhammar, 1999; Tzoulas et al., 2007). The Biophilia Hypothesis posits that humans have an innate desire to connect with nature, suggesting that urban green spaces fulfill this need and promote mental health by reducing stress and enhancing cognitive functioning (Wilson, 1984; Kellert & Wilson, 1993; Ulrich et al., 1991).

The benefits of urban green spaces extend to critical ecosystem services that combat the Urban Heat Island (UHI) effect and foster biodiversity. They moderate temperature increases through shading and evapotranspiration, contributing to a cooler urban environment and reducing energy consumption (Oke, 1989; Bowler et al., 2010). Additionally, urban green spaces enhance social cohesion by providing areas for community interaction and recreational activities, which are linked to lower crime rates and improved mental well-being (Kuo et al., 1998; Kuo & Sullivan, 2001). Overall, these findings highlight the multifaceted advantages of integrating green spaces into urban planning to create healthier and more resilient urban environments.

2.2. Environmental quality

The concept of environmental quality within urban planning involves considering social, economic, cultural, physical, and emotional factors in both tangible and intangible aspects. Defining environmental quality is challenging due to its multi-dimensional, multifaceted, and interdisciplinary nature. Environmental quality and public health, particularly focusing on how environmental factors like pollution impact mental health, especially in children. Studies indicate that exposure to environmental chemicals, such as heavy metals and endocrine disruptors, correlates with increased risks of mood and anxiety disorders in children, highlighting the need for a deeper understanding of these impacts (Thoma et al., 2021). Numerous studies have explored urban environmental quality, utilizing one or more parameters to measure the quality of the environment. Notably, the appropriate distribution of urban green space and vegetation density has been highlighted as a key factor in refreshing the air and, consequently, improving overall urban environmental quality (Faryadi & Taheri, 2008). Another perspective involves a spatiotemporal and qualitative examination. An index commonly utilized to assess the adequacy of urban greenery is the ratio of square meters of green spaces to the city's population (m2 green spaces / inhabitants) and the building block density (m2 green spaces / building density), which is considered as an indicator (Tsouchlaraki et al., 2010).

Over the past millennium, humans have increasingly played a significant role in altering the global environment. As the human population grows and technologies advance, mankind has become the most influential and widespread force driving environmental changes in the biosphere (Saied et al., 2004). In general, the density of housing stands out as a significant adverse predictor for the extent of green spaces and tree cover, as indicated by Richard et al. in 2008. Numerous studies have employed quantitative methods, qualitative descriptions, attitudinal explanations, and landscape assessments to explore this relationship. Despite these efforts, achieving a comprehensive understanding of urban environmental quality remains challenging and elusive.

This complexity necessitates the incorporation of various elements, as relying on a single or a few indicators alone proves insufficient for gauging environmental quality accurately. Recognizing this, numerous studies advocate for an integrated approach to the topic. Some even argue for the inclusion of diverse perspectives, incorporating local knowledge about neighborhood aspects and conditions into environmental assessments. However, (Liang & Weng, 2011) highlight a major obstacle in urban environmental quality research—the absence of a straightforward method to model and predict the interactions among all these aspects and variables.

2.3. Urban greenery

Green spaces are vital components of urban environments, encompassing parks, gardens, and natural landscapes that contribute significantly to environmental quality and public health. Defined as areas primarily covered with vegetation, these spaces provide essential ecosystem services such as air purification, water filtration, temperature regulation, and noise reduction. Their role in improving air quality has been extensively documented, with research showing that vegetation helps absorb pollutants, thus reducing respiratory issues among urban populations (Bolund & Hunhammar, 1999; Tzoulas et al., 2007). Additionally, urban green spaces are linked to enhanced mental well-being, offering opportunities for relaxation and social interaction, which are crucial for fostering community cohesion (Wilson, 1984; Kaplan & Kaplan, 1989).

The benefits of urban green spaces extend beyond individual health to encompass broader ecological and economic advantages. They play a critical role in biodiversity conservation by providing habitats for various species and serving as corridors for wildlife movement. Green spaces can also enhance property values and stimulate local economies, making them attractive areas for residents and businesses alike (Chiesura, 2004). Furthermore, these spaces help mitigate the Urban Heat Island (UHI) effect by regulating temperatures through shading and evapotranspiration, contributing to overall urban sustainability (Oke, 1989; Bowler et al., 2010).

Despite their numerous advantages, urban green spaces face significant challenges. Rapid urbanization often leads to land use pressure, with green areas being converted into commercial or residential developments, which undermines their ecological benefits (Zhao et al., 2016). Maintenance and funding issues can result in neglected green spaces, diminishing their accessibility and quality (Floyd, 2010). Additionally, inequitable access to these areas can exacerbate social disparities, limiting the benefits for marginalized communities (Wolch et al., 2014). Addressing these challenges is essential to maximize the potential of green spaces and ensure that all urban residents can enjoy their multifaceted benefits.

2.4. Geospatial Approach

The geospatial approach is a technique that considers the Earth's specific locations in its analysis. It explicitly incorporates the geographic coordinates, and the outcomes offer crucial insights into comprehending the impact of changes when the locations of the phenomena under scrutiny are altered. Geospatial methods encompass a diverse array of numerical techniques within their broader classification (Cromley, 2013).

2.4.1. Spatiotemporal Approach

Another method involves a spatiotemporal and qualitative examination. An index commonly employed to assess the adequacy of urban greenery is the ratio of square meters of green spaces to the city's population and building density. This is expressed as m2 of green spaces per inhabitant and m2 of green spaces per density of building block, as proposed by Tsouchlaraki et al. in 2010.

2.4.2. Geographic Information System

A geographic information system (GIS) is a computerized tool designed for the mapping and analysis of geographic phenomena and events occurring on Earth. The technology of GIS integrates standard database functions like querying and statistical analysis with the distinct benefits of visualization and geographic analysis offered by maps. These capabilities set GIS apart from other information systems, rendering it valuable across a wide spectrum of public and private enterprises for elucidating events, forecasting outcomes, and devising strategic plans. GIS for environmental monitoring, emphasizing their vital role in managing natural resources and enhancing environmental quality. (Zhang, Y., et al. 2023) highlight various case studies that showcase the successful implementation of GIS in urban planning and environmental assessments. By tracking environmental changes and informing decision-making processes, GIS emerges as a critical tool in addressing contemporary environmental challenges and promoting sustainability initiatives.

2.4.3. Weighted Overlay Approach

In his work "Design with Nature" (McHarg, 1969), Ian McHarg initially emphasized the importance of overlay methods for environmentally sensitive planning. The Weighted Overlay technique stands out as a widely employed approach in overlay analysis, particularly for addressing multi-criteria issues such as optimal site selection and the development of suitability models (Esri, 2013). This method aims to determine the most favorable locations for a specific phenomenon while applying a uniform set of values to diverse inputs, facilitating an integrated analysis. A fundamental aspect of Geographic Information Systems (GIS) involves the capability to overlay various layers of spatially referenced data (Akanbi et al., 2013). By utilizing the Weighted Overlay Method, the assessment of various factors for suitability in relation to a specific phenomenon becomes more nuanced. This is essential because these factors often possess distinct value scales and varying levels of importance in suitability models, preventing straightforward addition or direct comparison.

2.4.3.1. The Analytic Hierarchy Process (AHP)

The Analytic Hierarchy Process (AHP) was introduced by Saaty in 1980 as a multi-criteria decision-making approach. This methodology has garnered significant attention from researchers, primarily owing to its favorable mathematical properties and the ease of obtaining required input data, as noted by Triantaphyllou & Mann in 1995. Serving as a decision support tool, AHP addresses intricate decision-making problems through a multi-level hierarchical structure encompassing objectives, criteria, sub-criteria, and alternatives. The necessary data are acquired through a series of pair-wise comparisons. These comparisons are instrumental in determining the weights assigned to decision criteria and the relative performance measures of alternatives concerning each specific decision criterion. In cases where the comparisons exhibit inconsistency, AHP offers a mechanism for enhancing coherence. Notably, the AHP, with its utilization of pair-wise comparisons, has been influential in the development of various other decision-making methods.

2.4.3.2. Pairwise Comparison

Pairwise comparison emphasizes its relevance in decision-making processes, particularly within multi-criteria decision analysis. The study explores the uncertainties related to prioritization based on pairwise comparisons, addressing issues of consistency and credibility in prioritization results. Key findings highlight the implications of consistent and inconsistent pairwise comparison matrices (PCMs) on decision-making outcomes, particularly in establishing the reliability of priority vectors derived from these comparisons. This research underscores the need for improved methodologies to enhance prioritization quality in various applications (Smith, 2023).While numerous methods employing pairwise comparisons ultimately convert qualitative responses into numerical values, often as ratios of integers, correctly quantifying these comparisons remains the most crucial step in multi criteria decision making. Quantification of pairwise comparisons involves utilizing a scale—a one-to-one mapping between the discrete choices available to the decision maker and a discrete set of numbers representing the importance or weight assigned to each choice.

2.5. Metrics for Assessing Environmental Quality

2.5.1. Land use and land cover

Land use and land cover change, emphasizing the drivers behind these changes, such as socio-economic factors, environmental policies, and technological advancements. It offers a framework for understanding how LULC changes impact ecosystem services and environmental quality. The authors explore historical trends and project future changes using various models and scenarios, highlighting the importance of interdisciplinary approaches in LULC studies. (Meyer & Turner, 2021)

2.5.2. **Urban greenery and the density of vegetation**

Green spaces constitute a vital component within intricate urban ecosystems, offering a range of advantages such as environmental, aesthetic, recreational, and economic benefits to urban residents. The presence of vegetation plays a crucial role in cooling the environment by providing shade and facilitating increased evapotranspiration (Christian & Ugoyibo, 2013). Despite these benefits, the significance of urban green spaces and the density of vegetation have been underscored as key indicators for enhancing air quality, thereby contributing to an overall improvement in urban environmental conditions (Faryadi & Taheri, 2008).

2.5.3. **Temperature**

There is a clear correlation between temperature and environmental conditions, given that temperature serves as an indicator of urban environmental degradation. As urban temperatures rise, there is a likelihood of increased instances of social and environmental injustices within cities. Elevated thermal levels in urban areas are commonly viewed as a marker of subpar urban environmental conditions, a critical component in assessing urban environmental quality (Opeyemi & Trina, 2014).

2.5.4. **Population density**

The complexities of population density and its implications for urban dynamics. A study in Greece demonstrated how population density varies significantly across regions, impacting urban concentration and rural depopulation patterns. The research utilized geographically weighted regression models to understand these dynamics, emphasizing the need for localized data to inform effective regional management strategies (Li, Huang, Wang, & Zhang, 2023).

Additionally, population density influences public health, environmental quality, and urban planning. As urban areas become more densely populated, they face challenges related to infrastructure, resources, and environmental sustainability.Understanding these relationships is essential for policymakers aiming to balance urban growth with quality of life considerations (Hofmann & Rojas, 2022).

2.5.5. **Air Quality**

Elevated levels of carbon monoxide concentration within the sub-city are regarded as a human indicator of poor urban environmental quality. This parameter is significant in assessing the overall quality of the urban environment (Opeyemi & Trina, 2014).

2.5.6. **Density of built-up area**

The significance of built-up area density in shaping urban environments and their effects on environmental quality. Increased built-up area density is associated with challenges such as elevated air pollution levels and diminished access to green spaces. Consequently, effective urban planning is essential to mitigate these adverse effects while promoting sustainability(Wang et al., 2021).This indicates that the expansion of urban areas contributes to elevated temperatures by replacing natural environments (such as forests, water bodies, and pastures) with surfaces that do not facilitate evaporation or transpiration, such as stone, metal, and concrete. In general, the density of housing emerges as a significant adverse factor affecting the availability of green spaces and tree cover (Davies et al., 2008).

2.6. Applications of GIS and Remote Sensing

The integration of Remote Sensing (RS) techniques within the Geographic Information System (GIS) framework significantly reduces the time, effort, and costs associated with utilizing geographical data. Remote sensing, offering advantages such as spatial, spectral, and temporal data availability, efficiently covers expansive and challenging-to-reach areas in a short timeframe, making it a valuable tool for assessing, monitoring, and conserving urban green spaces. Satellite Remote Sensing, characterized by repetitive coverage and multi-spectral capabilities, emerges as a robust method for mapping and tracking emerging changes both in the central and peripheral zones of urban areas (Akanbi et al., 2013).Satellite images play a crucial role in enhancing our understanding of intrinsic components of ecosystems and interactions within the overall environment. The significance of remote sensing in evaluating urban environmental quality is further heightened by the integration of Geographic Information System (GIS), facilitating the combination of remote sensing data with socio-economic variables and in situ data (Opeyemi & Trina, 2014).

2.6.1. **Assessing green space through the use of the (NDVI)**

The use of NDVI for green space assessment and understanding its impacts on urban environments. NDVI remains a widely accepted metric for estimating vegetation density and health, benefiting urban planning, environmental health studies, and exposure assessments. For instance, one recent study employed high-resolution NDVI from sources like Sentinel-2 and Landsat to map urban green spaces and their relationship with public health outcomes, refining estimates of greenness exposure by analyzing various spatial resolutions and calculating buffer zones around urban sites (Jimenez et al., 2023)

Understanding information related to green spaces is crucial for analyzing the environmental quality in urban areas. Advanced tools such as Remote Sensing and GIS have become instrumental in assessing natural resources, creating maps, and predicting the percentage of greenery available in a given area (Saied et al., 2004). Traditionally, estimating or extracting green percentages was a time-consuming and inaccurate process, especially for large areas. This conventional approach was tedious, consumed significant time, and incurred high costs. However, the advent of remote sensing techniques has revolutionized the process, particularly in differentiating and quantitatively measuring urban green spaces. The measurement of NDVI through remote sensing techniques provides a comprehensive view of all existing vegetation in green land areas. NDVI serves as an effective tool for assessing vegetative cover across extensive regions. It highlights dense vegetation in imagery, making it easily distinguishable from areas with little or no vegetation. Additionally, NDVI can identify water surface areas. Vegetation stands out from other land surfaces because it strongly absorbs red wavelengths of sunlight and reflects near-infrared wavelengths. NDVI values range between -1 and 1, where values around 0.5 indicate dense vegetation, values below 0 suggest the absence of vegetation, and healthy vegetation tends to absorb more visible light while reflecting a substantial portion of near-infrared light.

2.7 Urban Green Spaces and Sustainable Living Standards

Urban green spaces in promoting sustainable living standards, as these areas are crucial for environmental quality, social cohesion, and public health. Urban green spaces, which include parks, green corridors, and community gardens, provide vital ecosystem services such as air purification, climate regulation, and water management, which enhance urban resilience to climate change and pollution (Bolund & Hunhammar, 1999). These spaces support sustainable urban development by improving the quality of life, reducing heat in densely built areas, and promoting mental well-being, all of which contribute to healthier and more sustainable urban environments (Tzoulas et al., 2007).

The concept of sustainable living standards is also supported by frameworks like the United Nations' Sustainable Development Goals (SDGs), which highlight the importance of accessible green spaces for inclusive, safe, and resilient cities (UN-Habitat, 2020). Research indicates that access to green spaces reduces stress, encourages physical activity, and strengthens social ties, which collectively foster a sense of community and well-being essential for sustainability (Kabisch et al., 2015).

2.8. Empirical review

(Knobel Guelar, 2020) study explored the impact of urban green space quality on human health, addressing the gap in existing research that primarily focused on the presence of green spaces rather than their quality. Recognizing the growing urban population and the accumulating evidence of green spaces' health benefits, Guelar aimed to assess how green space quality influences the relationship between urban green spaces and human health. The study involved a systematic review of tools to assess green space quality, the development of a new assessment tool called RECITAL, and its application in Barcelona to examine the link between green space quality and health outcomes like physical activity and obesity. The research also compared different green space exposure metrics and their association with cardiovascular risk factors in Philadelphia. The findings highlighted the importance of green space quality and measurement methods in understanding the health benefits of urban green spaces, with social, demographic, and economic factors also influencing this relationship.

Similarly, (Daniels et al., 2017) studied urban green space structures from a multidimensional perspective. They highlighted the importance of designing green spaces in compact cities to address ecological, microclimatic, and recreational needs. The study identified shortcomings in current green space assessment methods and advocated for a more detailed evaluation, distinguishing between natural and artificial elements. Their integrated analysis revealed significant differences in evaluations between perspectives and between natural and artificial elements. The findings suggested the need for integrative planning that considers the varied contributions of green space elements and emphasizes a holistic approach to assessment and planning.

(Lam, Ng, Hui, & Chan, 2005) studied the environmental quality of urban parks and open spaces in Hong Kong. They explored the effectiveness of these areas in improving urban environments by assessing air quality, noise levels, and heavy metal contamination. Using a combination of field measurements and computer simulations, they discovered that while air quality in parks was better than at roadways, it was not significantly different from ambient levels. Noise levels in parks were similar to those in typical home environments, and heavy metal contamination in park dust was slightly lower than at roadways but comparable to home and school environments. The study suggested that urban parks' ability to enhance environmental quality in densely populated cities is limited and highlighted the need for better design and management of these spaces to improve urban livability.

Similarly (Assaye, Suryabhagavan, & Balakrishnan, 2017) explored the impact of urban green space on environmental quality in Addis Ababa. They found that unsustainable urban development had led to worsening environmental conditions, affecting natural vegetation, climate, wetlands, and wildlife. The study emphasized the importance of regular updates on urban environmental quality (UEQ) for effective urban planning. They used remotely sensed images and socio-economic data to analyze changes in environmental quality from 1986 to 2015, incorporating factors such as land use, surface temperature, and vegetation. Regression and factor analysis revealed four key factors: greenness, overcrowding, heat islands, and greenhouse gas emissions. By weighting these factors, they created a risk map and an index to assess changes in urban greenness as a measure of environmental quality.

Previous research at both global and national levels has utilized geospatial techniques to assess and analyze environmental quality and urban green spaces, though methodologies and findings have varied. Some studies have relied on outdated data and software for evaluating urban green spaces (UGS) and environmental quality (EQ). Additionally, administrative boundaries have changed since earlier studies: the area of Addis Ababa was 527 km^2 with 10 sub-cities in past research, but it is now 430 km^2 with 11 sub-cities. There have also been dynamic changes in land use and land cover in the area. This underscores the necessity for a more refined understanding of the geospatial dynamics impacting urban green spaces and their implications for environmental quality within the city. Consequently, this study seeks to address these gaps by integrating various geospatial software tools.

CHAPTER III: METHODOLOGY

3.1. Description of the Study Area

3.1.1. Location

Addis Ababa, the largest city and capital of Ethiopia, was one of the major urban centers on the African continent. The city was organized into 11 boroughs, known as sub-cities: Addis Ketema, Akaky Kaliti, Arada, Bole, Gullele, Kirkos, Kolfe Keranio, Lemi Kura, Lideta, Nifas Silk-Lafto, and Yeka, along with 116 weredas. It spans a total area of 430.26 km². As a key hub for transportation, coordination, commerce, banking, and insurance, Addis Ababa hosts numerous international organizations, including the Organization of African Unity. The city is situated at latitude between 08°51' and 09°05' N, and a longitude between 38°39' and 38°54' E.

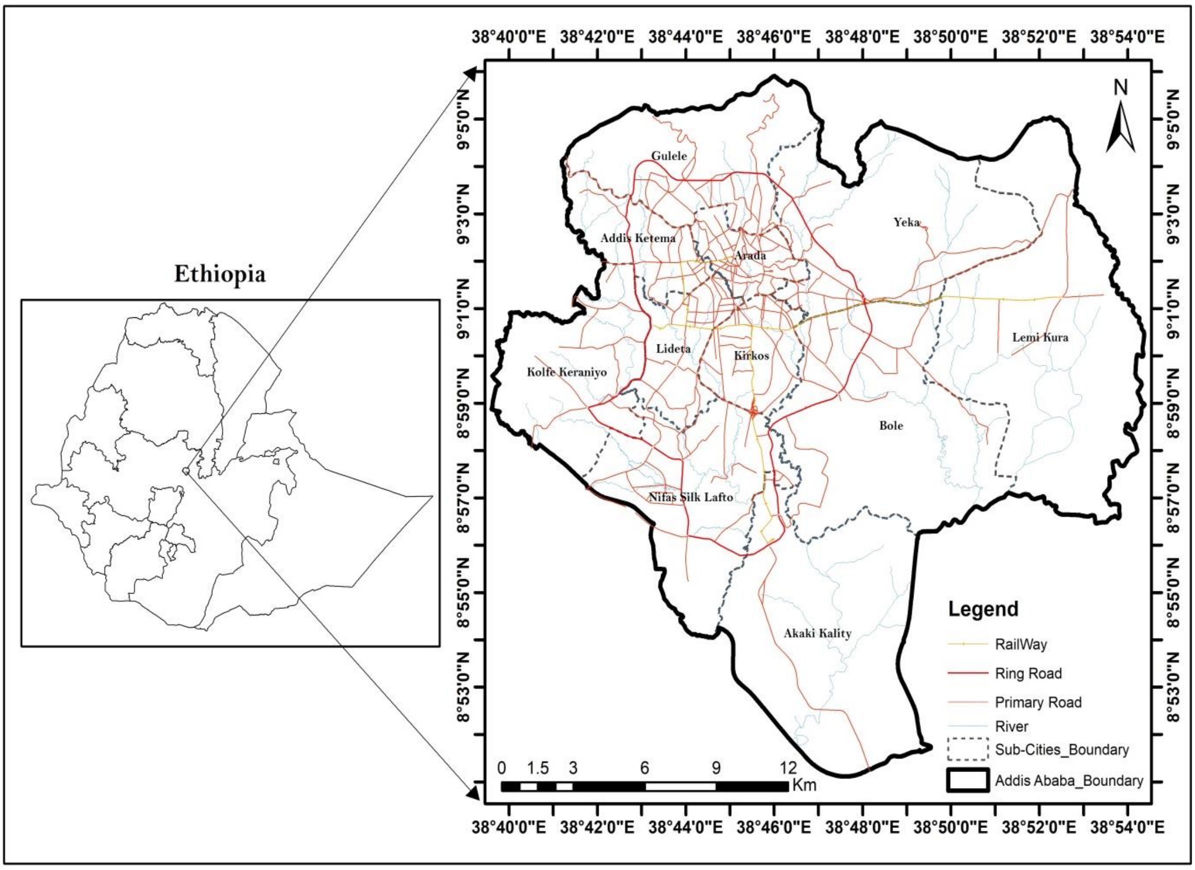

Figure 3.1 Study area map.

3.1.2. Topography

The study area exhibit a diverse range of elevations, varying between 2,020 meters and 3,030 meters above mean sea level. The southern region, including the Akaki Kality area, has a lower elevation, whereas the northern part, which encompasses Mount Entoto, features a higher elevation. In contrast, the central region of the study area has a moderate elevation relative to the other areas. The elevation map of the study area, based on SRTM 20m data sourced from the USGS Earth Explorer website, is shown in Figure 3.2.

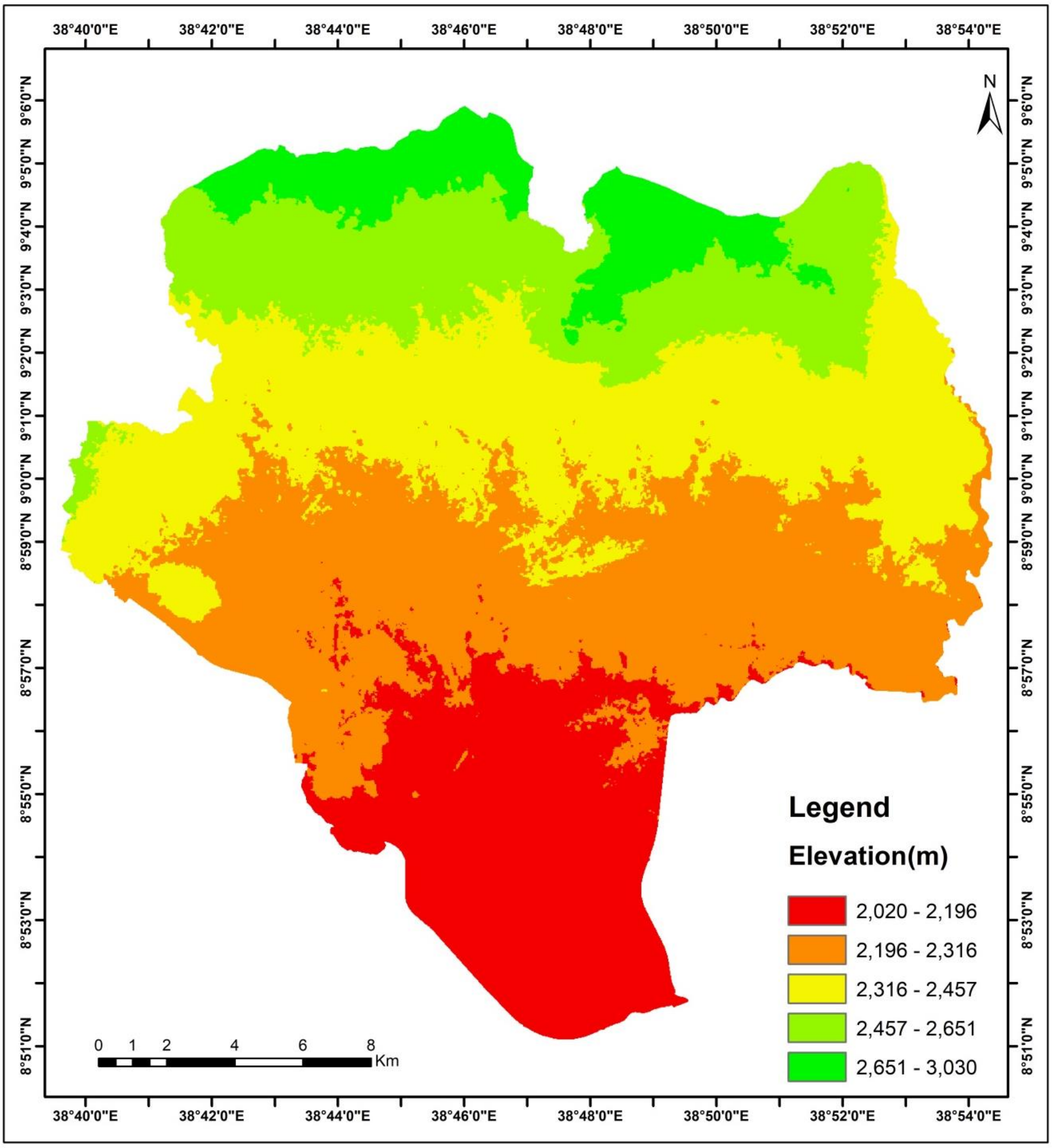

Figure 3.2 Study area elevation map

3.1.3. Climate

I. Rainfall

An extensive analysis of rainfall data from 1993 to 2023, sourced from various meteorological stations including Addis Ababa Bole and Addis Ababa Obs, reveals an average annual precipitation of 1209.56 mm. August recorded the highest monthly average rainfall at 268.98 mm, as shown in Figure 3.3. The primary rainy season generally spans March through September, with the peak period being from June to August. Conversely, January, February, October, November, and December are typically dry. Temperature patterns indicate that May is usually the warmest month, while July is typically the coolest. Among all months, January consistently experiences the lowest rainfall.

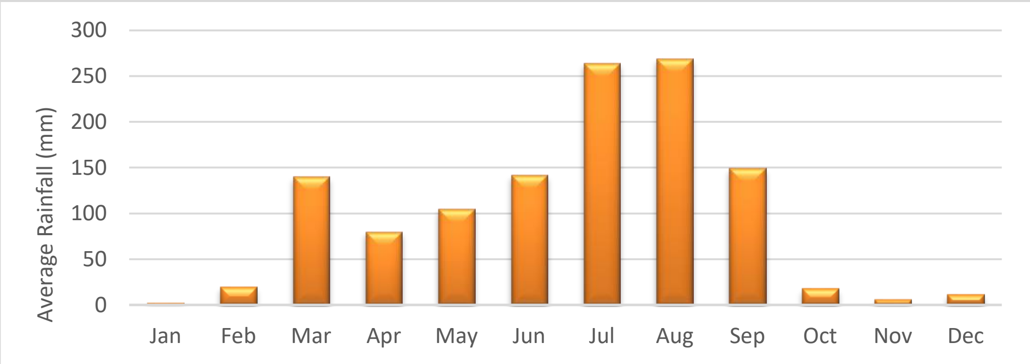

Figure 3.3: Distribution of the average monthly rainfall in the study area.

II. Temperature

The average annual temperature in Addis Ababa City is 25.21°C. The city's subtropical climate is shaped by its altitude, with areas ranging from 1,920 to 3,030 meters above sea level. May is the hottest month in the study area, with an average peak temperature of 29.5°C. Additional information is illustrated in Figure 3.4.

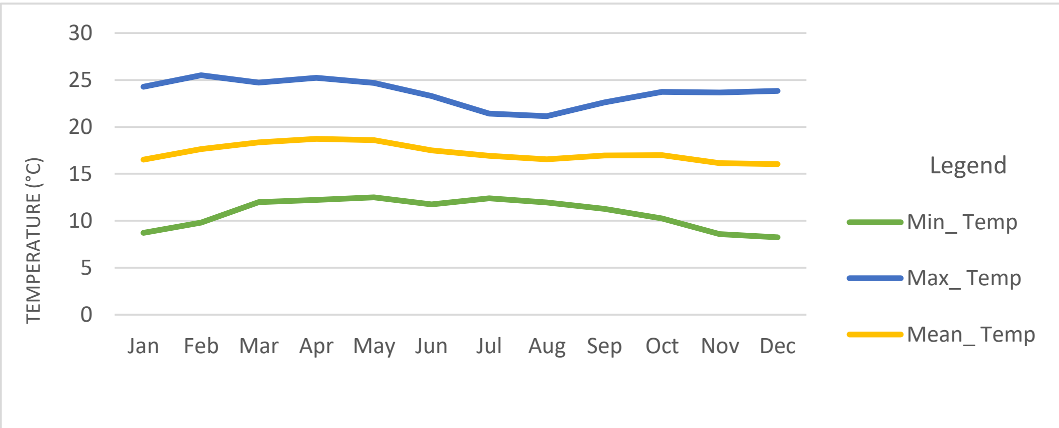

Figure 3.4: Maximum, mean and Minimum Monthly Temperature during 1993–2023.

3.1.4. Population

The population of Addis Ababa city in 2007 was two million seven hundred thirty-nine thousand five hundred fifty-one (2,739,551). After years, the population number increased by 158 % and reached four million three hundred twenty-seven thousand eight hundred forty-three (4,327,843) in the year 2023 projected (ESS, 2023).

Table 3.1: population of the study area by sub cities

	ESS projection (2023)			
Sub Cities	Male	Female	Total	Area(km^2)
Akaki Kaliti	126,473	134,494	260,967	66
Nefas Silk-Lafto	212,396	243,104	455,500	41.21
Kolfe Keraniyo	296,019	321,507	617,526	34.03
Gulele	184,471	200,861	385,332	36.37
Lideta	137,248	153,218	290,466	15.01
Lemikura	178,113	204,730	382,843	79.89
Kirkos	147,553	171,081	318,634	14.76
Arada	141,373	163,237	304,610	9.93
Addis Ketema	178,058	189,593	367,651	15.55
Yeka	230,371	268,930	499,301	53.91
Bole	207,037	237,976	445,013	63.59
Total population	2,039,112	2,288,731	4,327,843	430.25

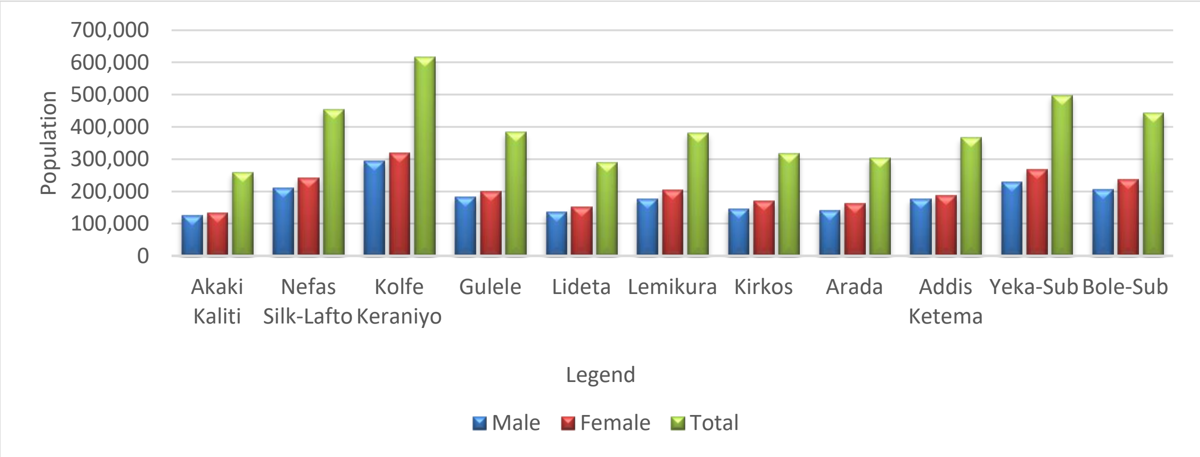

Figure 3.5: Population of study area

3.1.5. Soil

Soil results from the combined effects of climate, topography (including elevation, slope, and terrain orientation), biological activities (organisms), and parent materials (original rocks) interacting over time. According to the FAO soil classification, Addis Ababa features three soil types: chromic luvisols covering 79.83 km², pellic vertisols spanning 192.03 km², and eutric nitosols encompassing 158.35 km² (FAO, 2014).

3.1.6. Urban Attraction

Parks is a designated green space located in Addis Ababa, the capital city of Ethiopia. This park serves as an essential recreational area for both residents and visitors, offering a range of amenities including walking paths, playgrounds, sports facilities, and picnic areas. It significantly enhances urban life by providing a natural escape from the city's fast-paced environment, supporting ecological balance, and encouraging community engagement through various outdoor activities. Furthermore, the park frequently hosts cultural events, markets, and public gatherings, making it a lively hub for social and cultural interaction within the city.

Figure 3.6: Parks Located in study area

3.2. Research Approach and Design

This study utilized a quantitative, longitudinal research design to assess green space and environmental quality, focusing on changes over time. High-resolution, multi-temporal Landsat satellite imagery, along with supplementary data sources such as meteorological records, population statistics, and topographical maps, were collected to provide a robust dataset. Supervised classification techniques were applied to classify land cover types, followed by validation with ground truth data to ensure accuracy. Land Surface Temperature (LST) was extracted from the thermal infrared bands of the imagery and corroborated with on-site measurements. To analyze temporal changes in land use and land cover (LULC), change detection methods such as post-classification comparison and image differencing were employed. This comprehensive approach facilitated an in-depth understanding of how green space variations impact environmental quality, yielding valuable data to inform urban planning and environmental management strategies.

3.3. Data and software

This study employed a combination of primary and secondary data sources. The primary data, predominantly satellite imagery, was of utmost importance. Secondary data, also known as ancillary data, was obtained from a range of governmental and non-governmental organizations, as well as from published sources.

3.3.1. Primary data

The primary dataset consists of Landsat satellite imagery obtained from the USGS, including Thematic Mapper (TM) images from 1993, Landsat 7 ETM+ for the year 2003, as well as Operational Land Imager/Thermal Infrared Sensor (OLI/TIRS) images from 2014 and 2023. Additionally, a digital elevation model (DEM) with a 20m x 20m resolution was used to map the area's elevation. Field data, which includes GPS coordinates for different land use/land cover (LU/LC) classes, was also collected for verification purposes.

3.3.2. Satellite image data acquisition

Images from Landsat 5 TM for 1993, Landsat 7 ETM+ for 2003, and Landsat 8 OLI/TIRS for 2014 and 2023 were obtained. These cloud-free images, which cover the study area at path 168 and row 054, were downloaded from the Earth Explorer portal of the United States Geological Survey (USGS). The images are in the World Geodetic System 1984 (WGS84) projection. They were used to evaluate Land Surface Temperature (LST), Normalized Difference Vegetation Index (NDVI), and Land Use and Land Cover (LULC) in Addis Ababa, as detailed in Table 3.1.

Table 3.1: Satellite image used in the study.

Date of Acquisition YYYY/MM/DD	Sensor	Path	Row	Multispectral Band	Thermal Band	Spectral range(µm)	Spatial Resolution	Source
1993/03/13	TM	168	054	1 to5 and7	6	10.40-12.50	120m	USGS
2003/01/12	ETM+							
2014/01/18	OLI & TIR			1 to7 and9	10 and 11	10.60-12.51	100m	
2023/11/27								

I. Landsat Thematic Mapper (TM)

The Thematic Mapper (TM) sensor, which operated from March 1, 1984, to June 5, 2013, was installed on a satellite that orbited every 16 days. This sensor includes seven spectral bands: three in the visible range and four in the infrared range. Band 6, in particular, is specialized for detecting thermal infrared radiation and is used to measure surface temperatures. Detailed information is found in Table 3.2.

Table 3.2: Description of Landsat 5 thematic mapper.

Sensor	Band	Band name	Wavelength (µm)	Resolution (m)	Repeat cycle
Landsat5	1	Visible Blue	0.45 – 0.52	30	
Thematic	2	Visible Green	0.52 – 0.60	30	
Mapper	3	Visible Red	0.63 – 0.69	30	16 days
(TM)	4	NIR	0.76 – 0.90	30	
	5	SWIR 1	1.55 – 1.75	30	
	6	Thermal	10.40 – 12.50	30(120)	
	7	SWIR 2	2.08 – 2.35	30	

II. Landsat 7 Enhanced Thematic Mapper plus (ETM+)

The Landsat 7 satellite, equipped with the Enhanced Thematic Mapper plus (ETM+) sensor, has been capturing near-continuous Earth imagery since July 1999, following a 16-day repeat cycle. The Landsat 7 ETM+ provides images across eight spectral bands, with a spatial resolution of 30 meters for bands 1 through 5 and 7. The thermal band 6 has a resolution of 60 meters, while the panchromatic band 8 has a resolution of 15 meters. Detailed information is provided in Table 3.3.

Table 3.3: Description of Landsat 5 enhanced thematic mapper plus.

Sensor	Band	Band name	Wavelength (µm)	Resolution (m)	Repeat cycle
Landsat7	1	Visible Blue	0.45 – 0.52	30	
Enhanced	2	Visible Green	0.52 – 0.60	30	

Thematic	3	Visible Red	0.63 – 0.69	30	16 days
Mapper	4	NIR	0.77 – 0.90	30	
Plus	5	SWIR 1	1.55 – 1.75	30	
(ETM+)	6	Thermal	10.40 – 12.50	30(120)	
	7	SWIR 2	2.09 – 2.35	30	
	8	Band 8 - Panchromatic	0.52 – 0.90	15	

III. Landsat 8 operational land imager and thermal infrared sensor Capabilities

The images include nine spectral bands: bands 1 through 7, 9, and the thermal infrared sensor (TIRS) with bands 10 and 11, all featuring a spatial resolution of 30 meters. The newly introduced band 1, also referred to as ultra-blue, is particularly useful for analyzing coastal regions and aerosols. Band 9 is effective for detecting cirrus clouds. Landsat 8, which was launched on February 11, 2013, as shown in Table 3.4, is equipped with the OLI sensor. This sensor is designed to capture high-resolution imagery across various spectral bands, ranging from visible to near-infrared and shortwave infrared.

Table 3.4: Descriptions of Landsat 8 OLI and TIRS

Sensor	Band	Band name	Wavelength (μm)	Resolution (m)	Repeat cycle
	1	Coastal	0.43 – 0.45	30	
	2	Blue	0.45 – 0.51	30	
Landsat8	3	Green	0.53 – 0.59	30	
OLI/TIRS	4	Red	0.63 – 0.67	30	
	5	NIR	0.85 – 0.88	30	
	6	SWIR 1	1.57 – 1.65	30	16 days
	7	SWIR 2	2.11 – 2.29	30	
	8	Pan	0.50 – 0.68	15	
	9	Cirrus	1.36 – 1.38	30	
	10	TIRS 1	10.60 – 11.19	30 (100)	
	11	TIRS 2	11.50 – 12.51	30 100)	

3.3.3 Field data

The study employed field data obtained from GPS coordinates to accurately validate the classified land use/land cover (LU/LC) image across various categories. GPS points, selected at random, were collected along with photographs representing different LU/LC classes. This field data was crucial for assessing the accuracy of the classification, with the validation process relying on ground truth verification.

3.3.4. Secondary data

This research utilized secondary data, such as meteorological records including average monthly temperatures and rainfall spanning from 1993 to 2023, which were applied for both assessment and validation. The study also integrated a geological map sourced from the Geological Institute of Ethiopia to evaluate the geological features of the region. Furthermore, population data from the Ethiopia Statistical Service (ESS) from 2007 were analyzed to understand the demographic conditions within the study area.

3.3.5. Description of data and data source

The data used in this study, comprising both primary and secondary sources, was obtained from multiple locations as outlined in Table 3.5.

Table 3.5: Description of Data and data sources

No	Data Type	Data Sources
1	Boundary of the study Area	SSGI
2	Existing road	ERA
3	Landsat image (1993,2003,2014 & 2023)	USGS
4	Air Quality	AEPA
5	Population	ESS
6	Temperature and Rain fall	NMA

3.3.6. Software Packages and Instruments

Table 3.6: Software packages and Instruments used

Software packages	Purposes
ArcGIS Pro	Data analysis and map preparation
ERDAS IMAGINE 2015	For LULC classification and LST retrieval
Google Earth Pro	For reference in accuracy assessment
Quantum GIS 3.10	For downloading and processing Landsat Data
IDRISI 17	weight overly analysis
Handheld GPS	To collect ground truth data for accuracy assessment
Microsoft Office 2016	For statistical Data analysis and presentation

3.4. Methods

In this study, the methodology for achieving the research objectives began with acquiring Landsat images from the Earth Explorer website (USGS) for the years 1993, 2003, 2014, and 2023. These years were chosen based on data availability. The images were collected during the dry season and were cloud-free.

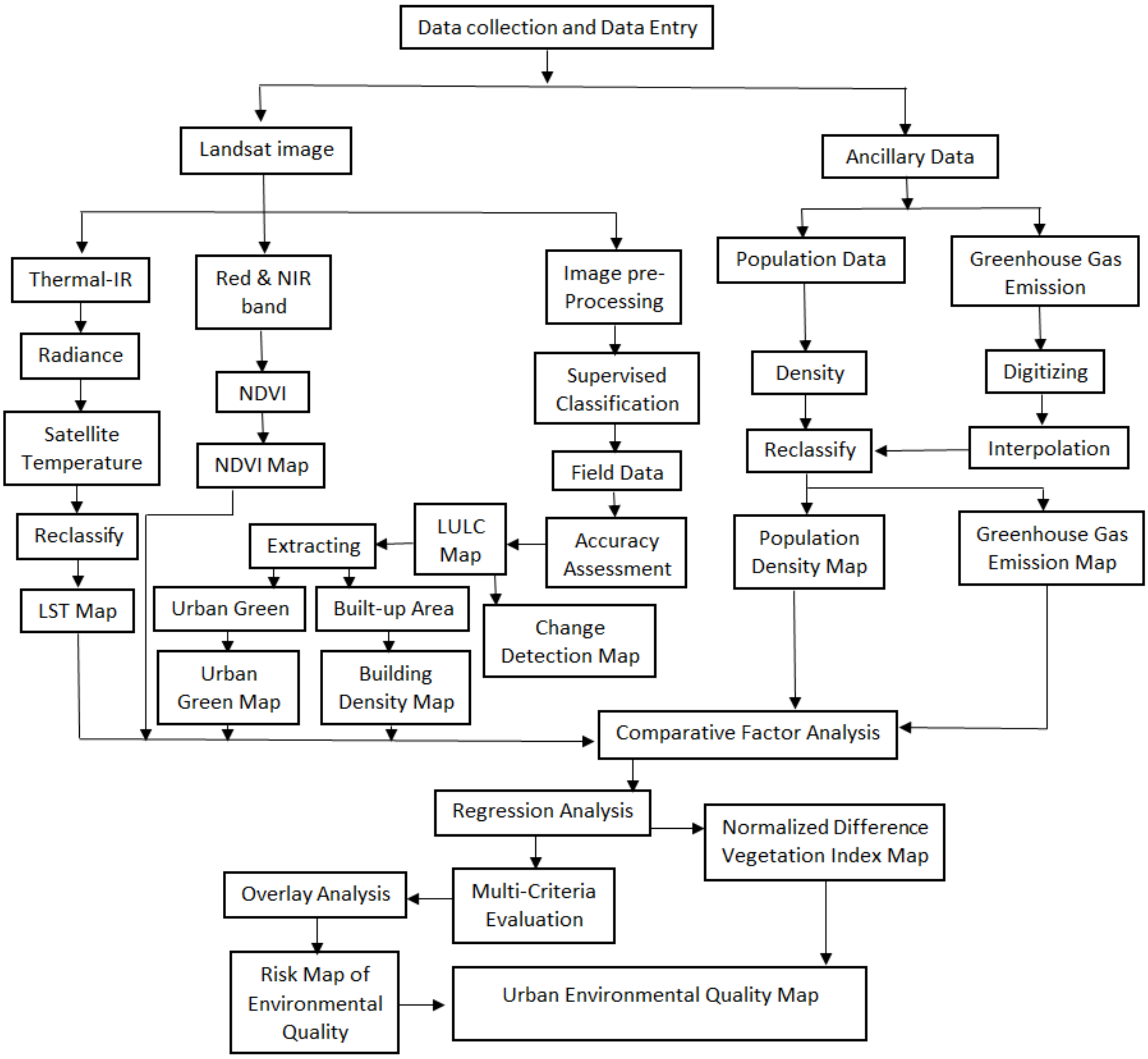

Figure 3.7 Methodological flow chart of the study.

3.4.1. Preparing and Analyzing Data

Satellite images often contain imperfections like distortion, noise, haze, and striping, which necessitate preprocessing before further analysis. The preprocessing steps included importing the images, stacking layers, and cropping them to match the boundaries of Addis Ababa city. This was followed by geometric and radiometric corrections, stripe removal, pan sharpening, and other enhancement techniques to improve image quality. Radiometric correction, in particular, helps remove atmospheric noise, allowing the sensors to better capture true ground conditions. These steps were crucial for enhancing the image's clarity and detail, making it easier to identify different features in the scene.

3.4.2. Processing of Digital Images

A digital image is fundamentally a numerical representation composed of binary data, capturing a two-dimensional visual scene. This image is formed by sampling and quantizing the scene into discrete elements called pixels. Digital Image Processing (DIP) encompasses the methods employed to manipulate and analyze these images using computers. In the realm of remote sensing, DIP has traditionally concentrated on two main applications: enhancing image quality for better visual interpretation by humans and optimizing image data for computer-assisted interpretation. The primary goal of DIP is to enhance the spectral characteristics of objects within the image for improved distinction.

3.4.3. Image enhancement

Image enhancement involves altering image data to improve its display or recording, making it more suitable for visual analysis. This often includes techniques that increase the visual contrast between various elements in an image (Billah and Rahman, 2004). The main objective of image enhancement is to make the information in images clearer for human viewers or to prepare the data for further automated image processing tasks.

3.4.4. Image classification

In remote sensing, the goal of image classification is to extract thematic information from a multi-band image by sorting it into distinct information categories. This process involves analyzing the image based on the reflectance properties of various objects to meet specific objectives, essentially converting image data into thematic groups. Digital image classification techniques categorize pixels into land use/land cover (LU/LC) classes based on their reflectance statistics. Pixels are grouped into clusters according to their reflectance characteristics, with users determining the desired number of clusters and selecting the spectral bands for analysis. The image classification software then generates these clusters based on the provided parameters. In this study, supervised classification techniques are used.

I. Supervised classification

Supervised classification is a widely used technique in the quantitative analysis of remote sensing (RS) imagery, based on the reflectance characteristics of the data. This approach uses spectral signatures from selected training samples to categorize the images. The image classification Toolbar assists in creating these training samples, which represent different classes. Through supervised classification, specific information classes, such as various types of land cover, can be identified within the image. Each year, the process involves classifying pixels by applying training areas for each land use/land cover (LU/LC) class. Once these training areas are defined, the classification is carried out. For LU/LC categories such as bare land, cropland, shrub land, built-up areas, forests, and water bodies, 10 training sites are selected. These areas in the digital images are labeled as signatures that represent distinct identities, and field truth verification is used to accurately reflect the LU/LC classes (Coppin & Bauer, 1996).

Using Bands 1 to 5 and 7 from the Multispectral Bands of TM and ETM+ for the years 1993 and 2003, along with Bands 2 to 7 from OLI for 2014 and 2023, the land-use and land-cover (LULC) patterns were identified through supervised classification with the likelihood classification algorithm in ERDAS Imagine 2015. In this approach, LULC classes were defined by the user using image processing techniques. The study identified six primary LULC classes in Addis Ababa: cropland, bare land, built-up areas, shrub land, forest land, and water bodies. Supervised classification provided advantages such as the creation of specific information classes, self-assessment using training sites, and the ability to reuse these sites for further analysis. However, challenges included discrepancies between information and spectral classes and variations in the homogeneity and uniformity of the information classes.

II. Maximum likelihood classification

Maximum Likelihood Classification (MLC) is a well-known technique in remote sensing used to assign pixels to specific classes or categories based on their statistical probabilities. This method, which relies on statistical decision-making, is especially effective for classifying pixels with overlapping spectral signatures, placing each pixel in the class where it has the highest probability of belonging. Although MLC is typically more accurate than parallelepiped classification, it demands more computational time. The MLC process also considers the variances within class signatures when determining the appropriate class for each pixel, as outlined in the signature file.

III. Ground truth

A ground truthing exercise was conducted in the study area to verify different land use and land cover (LU/LC) categories. The observed LU/LC classes included cropland, shrub land, forest, water bodies, bare land, and built-up areas, which were essential for creating the map legends. Using GPS technology, training datasets required for image classification were gathered. During these ground truthing activities, photographs and coordinates of particular scenes representing the sampled LU/LC classes were also recorded.

3.4.5. Classification accuracy assessment

Assessing the accuracy of a classification requires collecting original data or having existing knowledge about specific terrain areas for comparison. This involves comparing the classification map obtained through remote sensing with a reference map that is considered accurate, though it may still contain some errors.

The map, which is presumed to be accurate, may have been created either through direct on-site inspections or, more commonly, by analyzing remote sensing data collected at a higher scale or resolution. To assess its accuracy, this map is compared with a reference map derived from different data sources. A field survey, using handheld Global Positioning System (GPS) devices, identified around 60 points within the study area. This survey, along with Google Earth, was used to evaluate the accuracy of the Land-use/Land-cover (LU/LC) classification. The various land-use and land-cover classes are outlined in Table 3.7.

Table 3.7: Description of the study area land use/land cover class.

LU/LC classes	Code	Description
Shrubs Land	SL	Regions filled with shrubs, bushes, and small trees that offer minimal usable timber, interspersed with patches of grass and less than dense forests.
Crop Land	CL	Regions utilized for the farming of both annual and perennial crops, as well as the surrounding rural areas.
Built-up	BU	Regions utilized for residential, commercial, and industrial buildings, including areas designated for transportation such as roads, mixed-use urban developments, and other infrastructure.
Water Body	WB	Regions encompassing small natural and artificial dams, such as ponds, lakes, and rivers.

Forest Land	FL	A forest is an area densely populated with trees and serves as a natural habitat for diverse forms of life such as plants, animals, and microorganisms.
Bare land	BL	Regions characterized by thin soil, sand, and rocks, encompass deserts, dry salt flats, beaches, sand dunes, exposed rock formations, strip mines, quarries, and gravel pits. These areas are largely dominated by rocky outcrops, and lands that have been eroded or degraded.

To identify and categorize the land use/land cover (LU/LC) in the study area, having prior knowledge of the region is crucial. Field observations identified sex primary LU/LC classes. The classification process of LU/LC from a Landsat image is illustrated in Figure 3.8.

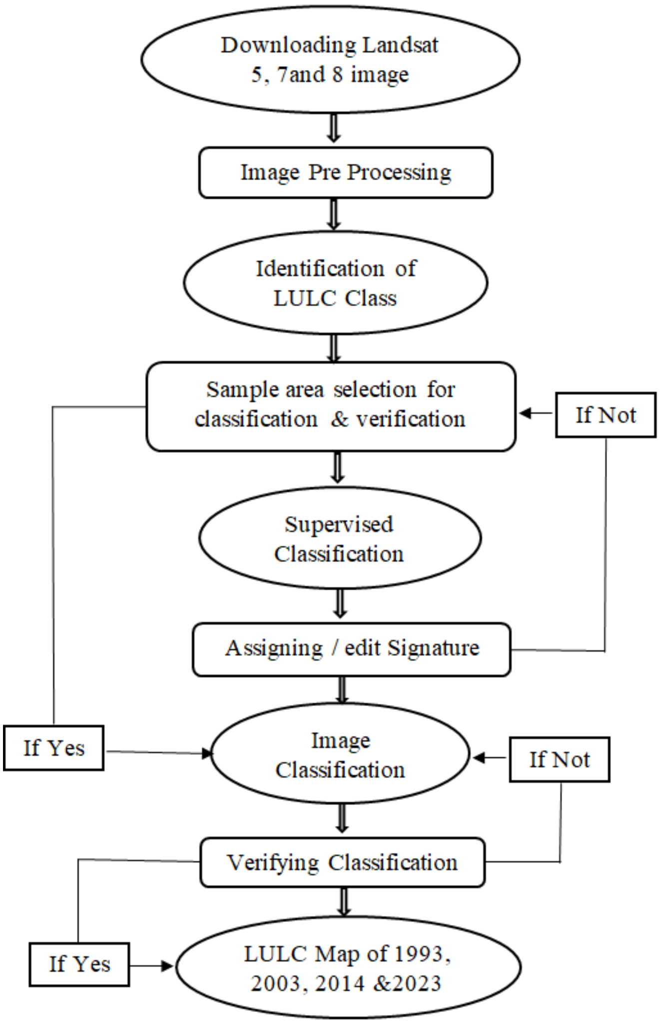

Figure 3.8: LU/LC Classification Procedures and methods used.

3.5. Land use and land cover change detection

Changes in land use and land cover (LU/LCC) were detected using satellite images from 1993, 2003, 2014, and 2023. The analysis was performed by employing GIS and the intersection method to compare thematic images from these years. The procedure began with mapping the most recent 2023 imagery and worked backward to 1993. According to Chen (2000), post-classification is a common technique for such change detection. The analysis utilized technical methods within ArcGIS to evaluate LU/LCC. A crucial aspect was the development of a table displaying the area in square kilometers and the percentage of change for each land use and cover class over the years 1993, 2003, 2014, and 2023, incorporating specific calculation formulas as described by Lambin et al. (2001) in Equation 3.1.

$$Percentage\ change = \frac{\text{observed change}}{\text{sum of area}} * 100 \qquad \text{Eq. (3.1)}$$

3.6. Vegetation Cover Distribution (Normalized Difference Vegetation Index)

Farooq (2012) describes that the Normalized Difference Vegetation Index (NDVI) is associated with vegetation presence, as areas with dense vegetation show a stronger reflection in the near-infrared spectrum. He highlights that green foliage reflects less than 20% of light in the 0.5 to 0.7 micrometer range but reflects approximately 60% in the 0.7 to 1.0 micrometer range. NDVI values, which range from -1 to 1, are calculated from spectral reflectance data in the visible (RED) and near-infrared (NIR) spectrums using ArcGIS Pro software. The index is derived from the following formula:

$$NDVI = \frac{\text{NIR}-\text{Red}}{\text{NIR}+\text{Red}} \qquad \text{Eq. (3.2)}$$

NDVI, or Normalized Difference Vegetation Index, utilizes specific spectral bands to calculate vegetation health. In this case, NIR refers to the near-infrared band (band 4) and Red refers to the red band (band 3). The calculation for NDVI is detailed in Equation 3.2, which applies to the TM sensor for 1993, the ETM+ sensor for 2003, and the OLI sensor for 2014 and 2023. For the Landsat 8 satellite, however, the NIR is band 5 and the red band is band 4, as described by (Weng et al. 2004).

3.7. Land Surface Temperature Extraction

In this study, the process involved converting the thermal bands from Landsat image thermal band, into radiance values, which were then used to calculate the satellite temperature. This temperature was adjusted using emissivity values derived from the Normalized Difference Vegetation Index (NDVI) to obtain the corrected satellite temperature. Finally, this corrected satellite temperature was converted into surface temperature. The procedure consisted of three main steps: first, transforming the digital number (DN) values from the thermal bands into spectral radiance; second, converting this spectral radiance into at-satellite brightness temperature (blackbody temperature); and third, adjusting this blackbody temperature to land surface temperature by accounting for emissivity variations caused by different land cover types.

3.7.1. Conversion of DN Values to Radiance

The OLI and TIRS band data were converted to Top-of-Atmosphere (TOA) radiance using the rescaling factors specified in the metadata file. The initial step involves converting the Digital Number (DN) values from the image into radiance units using equation. (3.3).

$$L\lambda = [ML * QCALMAX + AL] \qquad \text{Eq. (3.3)}$$

Where: Lλ= Top-of-Atmosphere (TOA) radiance (watts / (m² * srad* μm))

ML=Band-specific multiplicative rescaling factor from metadata

(RADIANCE_MULT_BAND_X, where X denotes the band number)

AL = Band-specific additive rescaling factor from metadata

(RADIANCE_ADDT_BAND_X, where X denotes the band number)

3.7.2. Conversion of Radiance to at Satellite Temperature

The next phase in quantitative analysis involves converting radiance into temperature. This calculation of satellite temperature is based on the assumption of a unit emissivity and employs the prelaunch calibration constants K1 and K2. Landsat 8 features two thermal bands, specifically bands 10 and 11. Calibration constants used for determining brightness temperature are detailed in Table 3.8.

Table 3.8: Thermal band calibration constant of Landsat 8.

Satellite	sensors	Categories	Band 10	Band 11
Landsat 8	OLI/TIRS	K1	774.8853	480.8883
		K2	1321.0789	1201.1442

$$TB = \frac{K2}{\left(Ln\frac{K1}{L\lambda}\right)+1} \qquad \text{Eq. (3.4)}$$

Where, TB: Effective brightness temperature of the satellite (measured in Kelvin)

K2: Calibration constant 2

Ln: Natural logarithm

K1: Calibration constant 1

Lλ: Spectral radiance at the sensor’s aperture

3.7.3. Estimation of Emissivity

Emissivity is crucial for accurate temperature measurements from the surface. In remote sensing, several methods have been developed to measure emissivity ($\boldsymbol{\varepsilon}$) from satellite data, considering that each pixel may be partially covered by vegetation and partially by soil or rock. The emissivity of each pixel is thus derived as a blend of the emissivity of these different surface types. One of the most effective models for this purpose is the Vegetation Cover Method (VCM) proposed by Valor et al. (1996), which provides the following operational equation (Equation 3.5).

$$\varepsilon = \varepsilon V\ PV + \varepsilon g\ (1 - PV)\ (1 - 1.74\ PV) + 1.7372\ PV\ (1 - P)$$

$$\varepsilon\ = 0.004\text{Pv} + 0.986 \qquad \text{Eq. (3.5)}$$

Where, "v" represents vegetation and "g" denotes ground. The fraction of cover, PV, can be directly derived from the NDVI vegetation index, which is obtained through satellite measurements.

$$Pv = \left(\frac{NDVI - NDVImin}{NDVImax - NDVImin}\right)^2 \qquad \text{Eq. (3.6)}$$

Where,

Pv= Proportion of Vegetation

NDVI= Normalize Difference Vegetation Index

NDVI min= Normalized Difference Vegetation Index Minimum Value

NDVI max= Normalized Difference Vegetation Index Maximum Value

3.7.4. Land Surface Temperature

Land Surface Temperature (LST) is subsequently determined using the emissivity values and the temperature measurements from the satellite, as outlined in Equation 6. This process yields an emissivity-corrected image as described.

$$TLST\ =\ TB\ 1 + W\ *\ (TB\ /\ \rho)\ *ln\ \varepsilon \qquad \text{Eq. (3.7)}$$

Where, TLST→ Surface temperature (K) TB= at satellite temperature

W = wavelength of emitted radiance (11.5 μm)

ρ=hc/k (1.438 x10−2)

h= plank’s constant (6.26 x10−34J-sec)

c= velocity of light (2.998 x108m/sec)

k= Stefan Boltzmann’s constant (1.38 x10−23J/K)

3.8. Population Density
Data on human population for each sub-city was sourced from the 2023 projections for Addis Ababa (ESS, 2023) and converted into a compatible shape file format. The population data was categorized based on settlement density, with high population density areas being designated as having poor environmental quality.

3.9. Air Quality
The carbon monoxide pollutant data was sourced from sample measurements provided by the Addis Ababa Environmental Protection Agency, which served as the baseline for the greenhouse gas (GHG) inventory, including carbon dioxide (CO_2), methane (CH_4), and nitrous oxide (N_2O). The inventory covered emissions from five sectors: stationary energy, transportation, waste, industrial processes and product use, and agriculture, forestry, and other land use. The raw data was digitized using the existing land-use/land-cover map, processed through interpolation methods, and then reclassified to identify areas with high GHG emissions that are considered environmentally critical.

3.10. Built-up Density
Rapid urbanization creates numerous issues due to its substantial demands on land, water, housing, transportation, healthcare, and education. This growth leads to several environmental challenges, partly driven by human activities like housing development (Twumasi & Mermen, 2006). For example, building density data from Addis Ababa's Integrated Land Information Center (2003) was obtained through shape files. This data was analyzed using the Raster Calculator tool in ArcGIS's Spatial Analyst extension, revealing high building density (see Fig. 3.7 in the general methodology).

Risk refers to the extent of potential total loss associated with a particular phenomenon due to various factors. Environmentally Critical Areas (ECA) is regions that include national parks, areas frequently exposed to hazards, or locations where a specific quality, property, or phenomenon experiences a significant change.

3.11. Parameter Criteria Classification and Map Generation
The next stage of the study was to determine the priority classes and influence for the weighted overlay operation. This study identified the following parameters (Table 4.3) as indicators of Urban Environmental Quality in the city of Addis Ababa. The evaluations for UEQ was conducted based on the six choose parameters land-use/land-cover, NDVI, surface temperature, building density, population density and greenhouse gas emission. Table 3.9 Reclassification for parameters value.

The subsequent phase of the study involved establishing priority classes and their impacts for the weighted overlay analysis. The research identified several parameters (as shown in Table 3.9) to gauge Urban Environmental Quality in Addis Ababa. The assessment of Urban Environmental Quality (UEQ) was based on six selected parameters: land use/land cover, NDVI, surface temperature, building density, population density, and greenhouse gas emissions.

Table 3.9 parameter values for the reclassification.

Parameters	Criteria	Unit	Urban Environmental Quality Indicator Rating			
			High	Moderate	Marginal	Not Suitable
Land Cover	LULC	Class	Forest land /Shrub land	Crop land	Water Body	Bare Land Built-up
	NDVI	Value	0.4 to 0.8	0.2 to 0.4	-1 to 0	0.2 to 0
NDBI	Built up Area	Density	<0.10	0.10-0.30	0.30-0.60	>0.60
Urban Heat	Surface Temperature	Value ^{0}C	17-25	25-27	27-29	>29
Population	Population size	p/km^2	<100	100-1000	1000-10000	>10000
Air Quality	Carbon emission	µg/m³	<50	50-100	100-150	>150

3.11.1. Development and Validation of the Urban Environmental Quality Index

The Land Cover categories identified were forest/shrub land, cropland, water bodies, Built-up, and bare lands. Risk variables such as population density, building density, thermal heat, and Air quality were utilized to create the Urban Environmental Quality (UEQ) index. Each component was weighted based on the percentage of variance it accounted for.

3.11.1.1. Model Validation Using Multi Regression Method

Accuracy assessment is essential to verify the effectiveness of the developed UEQ index. The overall accuracy for the four maps was 88. % for TM, 90% for ETM+, 91.67% and 90% for OLI_TIR. The land use (LU) map was created using a supervised maximum likelihood classifier. This study explored several approaches, including regression modeling, with the multiple regression method applied to validate the model through

Ordinary Least Squares regression, extending spatial analysis techniques. The GIS tool identified the original variables that correlated with the components under consideration as predictors, and a residual map was created with an adjusted R^2 of 94.8 Additionally, coefficient values were generated. The coefficient of determination was computed to assess the effectiveness of the developed regression models using the specified formula.

$$Y = \beta 0 + \beta 1X1 + \beta 2X2 + \cdots + \beta 0\beta 0 + \varepsilon \qquad \text{Eq. (3.8)}$$

Where, Y→ Dependent variable what you are trying to model or predict

X→ Explanatory variables you believe cause or explain the dependent variable

ß →Coefficients Values, computed by the regression tool, reflecting the relationship between explanatory variables and the dependent variable.

$\boldsymbol{\varepsilon}$ → Residuals the portion of the dependent variable that isn't explained by the model; under- and over-predictions.

3.11.1.2. Assigning Weight Values to Each Criteria Using the Analytic Hierarchy Process (AHP)

The Analytic Hierarchy Process (AHP) is a valuable, adaptable, and straightforward method used in scenarios where conflicting criteria complicate decision-making. Introduced by Saaty in 1980, AHP has since been applied across various scientific disciplines. The primary method for evaluating AHP involves a binary comparison approach, as described in Equation 3.9. This approach significantly simplifies the decision-making process by allowing for the simultaneous assessment of two components using IDRISI 17 software, with a weight consistency ratio of 0.04, indicating acceptable consistency (as per Equation 3.9). The criteria for the process were established based on multi-regression experiences, expert opinions, and information from diverse sources. Knowledge was further enhanced through discussions with students in relevant fields and reviews of authoritative literature.

$$CR = \frac{CI}{RI} \qquad \text{Eq. (3.9)}$$

Where CI →consistency index

$$CI = \frac{\lambda - n\,max}{\mathrm{n} - 1} \qquad \text{Eq. (3.10)}$$

$\lambda - nmax$ represents the principal eigenvalue of the matrix, while n denotes the matrix's order.

RI indicates the average consistency index derived based on the matrix's order. Using IDRISI17 software, the weights for each layer were assigned as detailed in Table 3.10, and the weight consistency ratio was 0.04, indicating that the consistency is acceptable.

Table 3.10 Weighting Value

No	Criteria	Weight %
1	Land-use/land-cover	21.05
2	Built up Density	17.34
3	Surface Temperature	17.95
4	Population Density	20.41
5	Air Quality	23.25

3.12. Integration of Environmental and Supplementary Data Variables

Correlation analysis, factor analysis, and overlay analysis were the primary methods used to combine environmental parameters from remotely sensed images with secondary data from census information. To highlight key urban environmental areas, a geospatial approach was employed using ERDAS Imagine, ArcGIS, and IDRISI software.

3.12.1. Regression Analysis

All five parameters extracted from the physical and secondary datasets were initially used to perform an ordinary least squares (OLS) correlation analysis. Appendix 4 presents the computed variables that were later identified as significant for the research. To evaluate their relevance to the study, the coefficients exhibited the expected signs, were statistically significant, showed no redundancy among explanatory variables, and the residuals were normally distributed and not spatially auto-correlated. Additionally, a strong Adjusted R-Squared value reflects their overall correlation with the evaluated variables.

3.12.2. Factor Analysis

For land-use/land-cover analysis in the study, the following methods were utilized: Maximum Likelihood Classification was employed for data processing, accuracy was assessed using 60 reference points, and the area in square kilometers for each land use/land cover type was calculated for each study year. These results were then compared across different years to evaluate changes.

3.12.3. Overlay Analysis

Overlay Analysis tools, available in the Spatial Analyst extension, are frequently employed to tackle multi-criteria problems, such as selecting optimal sites or modeling suitability. This technique involves applying a uniform scale of values to varied and disparate inputs, facilitating integrated analysis (Esri, 2013). It is particularly useful for identifying locations most at risk of environmental degradation. The initial step involved using ordinary least squares linear regression to model the operators and predict the dependent variable based on its relationships with a set of explanatory variables. Subsequently, an Environmental Quality risk map was created, which involved computing parameter layers by reclassifying variables such as population density, building density, urban heat, greenhouse gas emissions, and Land Use/Land Cover classification. These layers were then classified into different categories, with values assigned to each class, and the parameters were overlaid to create the final map. Table 3.9 provides a summary of the data groups, priority classes, point values, and influence (weight) values utilized for the weighted overlay process, which is essential for creating the final environmental risk map of the study area. This map integrates all these elements to depict the overall environmental quality in the region, reflecting the combined impact of all factors. In the weighted overlay method, environmental parameter layers are superimposed using a standardized measurement scale, with each layer weighted based on its significance.

Each cell within a layer is assigned a point value, calculated by multiplying the cell's priority class point by the influence factor of the associated secondary data group. The influence factors and updated cell values across secondary data layers are then multiplied to generate the environmental quality risk map. In addition to the weighted overlay technique, the Analytic Hierarchy Process (AHP) is a crucial tool for geographic analysis. It involves pair-wise comparisons and multi-criteria decision support to determine weighting factors, as summarized in Table 3.10 for the risk map assessing urban environmental quality.

A comprehensive integration of additional indicators is necessary to derive logical conclusions using deductive indices. For instance, the proportion of vegetation cover (NDVI index) and the risk map of environmental quality were combined through map algebra raster calculations to generate the Urban Environmental Quality result map shown in Figure 3.7. According to this index, areas with high greenhouse gas emissions, overpopulation, dense building structures, elevated heat levels, and low vegetation cover receive the lowest scores, marking them as critical zones. Conversely, regions with sparse population, low heat, minimal construction, low greenhouse gas emissions, and high vegetation cover are deemed to have suitable environmental quality.

CHAPTER IV: RESULTS AND DISCUSSIONS

4.1. Land-use/land-cover

The 1993 land-use/land-cover (LU/LC) classification showed that Cropland and Built-up areas were the most dominant, making up 74.01% of the total area. Specifically, Cropland covered 196.86 km² (45.76%), and Built-up areas occupied 121.55 km² (28.25%) of the 430.25 km² area. The remaining 111.83 km² (25.99%) was composed of bare land, forest, shrub land, and water bodies, with water bodies taking up the least space. By 2003, Built-up areas had become the most prevalent LU/LC type, spanning 175.07 km² (40.69%) of the area, while Cropland covered 139.10 km² (32.33%). The remaining land use/land cover (LU/LC) categories, such as bare land, shrub land, forest land, and water bodies, accounted for 26.98% of the landscape. In 2003, water bodies covered the least area among all categories. A study conducted in 2014 revealed that built-up areas dominated the landscape, covering 236.78 km², or 55.03% of the total area. Croplands were the next most significant category, encompassing 115.98 km², or 26.96%. The remaining classes, including bare land, forest land, shrub land, and water bodies, together made up 18.01% of the land, with water bodies once again occupying the smallest area among these classes.

The 2023 land use and land cover (LU/LC) classification revealed that built-up areas and cropland were the dominant categories, accounting for 86.43% of the total area. Built-up areas alone covered 257.12 km², or 59.76%, while cropland occupied 114.74 km², or 26.67%. The remaining 13.57% of the area was composed of bare land, forest, shrub land, and water bodies. It is notable that the cropland area decreased by 13.73% since 1993. Built-up areas continue to be the most extensive land use and cover type, followed by cropland. Detailed statistics and the LU/LC map for the period are presented in Table 4.1 and Figure 4.1.

Table 4.1: LU/LC analysis of the Study Area.

No	Land Cover Type	1993		2003		2014		2023	
		Area(km)	Area(%)	Area(km)	Area(%)	Area(km)	Area(%)	Area(km)	Area(%)
1	Water Body	1.26	0.29	0.98	0.23	0.99	0.23	1.53	0.35
2	Built-up	121.55	28.25	175.07	40.69	236.78	55.03	257.12	59.76
3	Shrub Land	27.37	6.36	68.02	15.81	28.79	6.69	9.65	2.24
4	Bare Land	36.01	8.37	6.91	1.61	6.21	1.44	0.67	0.16
5	Forestland	47.19	10.97	40.16	9.33	41.50	9.64	46.55	10.82
6	Cropland	196.86	45.76	139.10	32.33	115.98	26.96	114.74	26.67
	Total	430.25	100	430.25	100	430.25	100	430.25	100

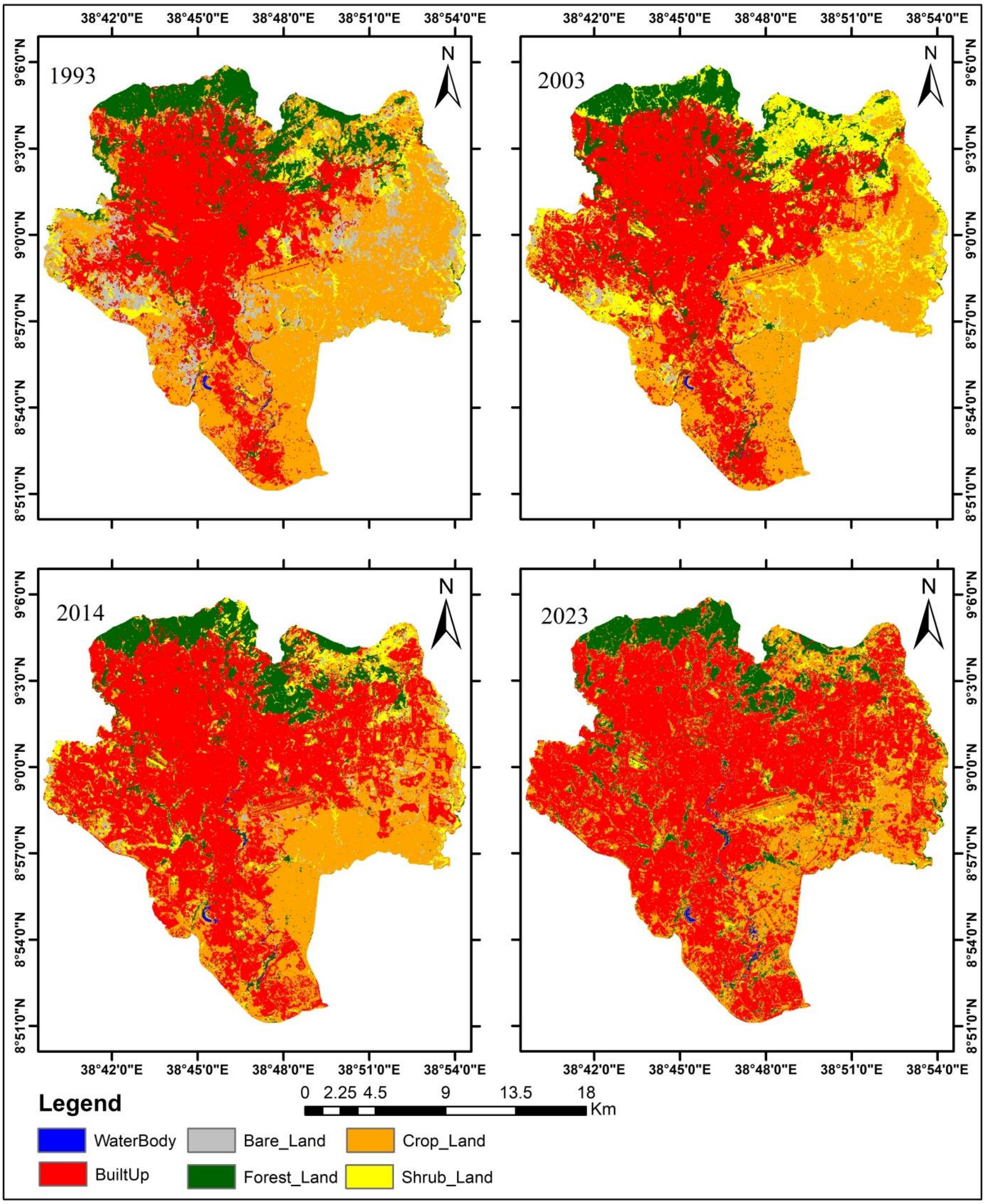

Figure 4.1: LU/LC maps of the study area.

Between 1993 and 2023, cropland has shown a continuous decrease in land use/land cover type in the study area. The built-up area, which was 121.55 km² in 1993, grew to 175.07 km² by 2003. It continued to expand, reaching 236.78 km² in 2014 and further increasing to 257.12 km² by 2023, as illustrated in Figure 4.2.

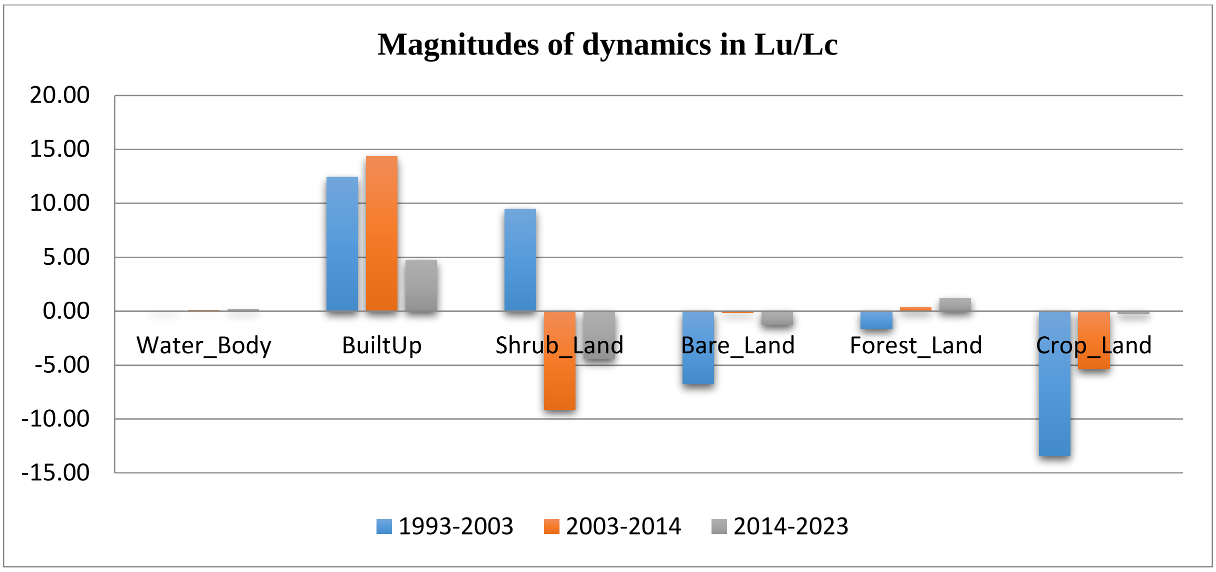

Figure 4.2: Magnitudes of dynamics of LU/LC.

4.2. Spatial extent of land-use/land-cover

The land-use and land-cover (LU/LC) patterns in the study area have undergone significant changes from 1993 to 2023. Throughout this period, Built-up areas and Crop Land consistently dominated more than 86% of the land across all six major LU/LC classes. The built-up area notably expanded from 28.25% in 1993 to 40.69% in 2003, then to 55.03% by 2013, and further to 59.76% by 2023. Water bodies fluctuated, starting at 0.29% in 1993, decreasing to 0.23% in 2003, remaining stable at 0.23% in 2014, and eventually increasing to 0.35% by 2023. The percentage of forested areas also varied, beginning at 10.97% in 1993, declining to 9.33% by 2003, rising to 9.64% in 2014, and reaching 10.82% by 2023.

Similarly, Shrub land percentages varied over time, starting at 6.36% in 1993, rising to 15.81% by 2003, then dropping to 6.69% in 2014, and further declining to 2.24% by 2023. Cropland initially decreased from 45.76% in 1993 to 32.33% in 2003, followed by another decrease to 26.96% in 2014, and continued to decline, reaching 56.64% by 2023. Bare land percentages consistently declined throughout the period from 1993 to 2023, starting at 8.37% in 1993, reducing to 1.61% by 2003, further decreasing to 1.44% in 2014, and slightly rising to 0.16% by 2023 (Table 4.2).

Table 4.2: Land-use/land-cover coverage and net changes during 1993–2023.

No	Land Cover Type	1993 Area (km)	1993 Area (%)	2003 Area (km)	2003 Area (%)	2014 Area (km)	2014 Area (%)	2023 Area (km)	2023 Area (%)	Net Change 1993-2023, Km2
1	Water Body	1.26	0.29	0.98	0.23	0.99	0.23	1.53	0.35	**0.26**
2	built-up	144.60	33.61	175.07	40.69	236.78	55.03	257.12	59.76	**135.57**
3	Shrub Land	27.37	6.36	68.02	15.81	28.79	6.69	9.65	2.24	**-17.72**
4	Bare Land	36.01	8.37	6.91	1.61	6.21	1.44	0.67	0.16	**-35.34**
5	Forestland	47.19	10.97	40.16	9.33	41.50	9.64	46.55	10.82	**-0.64**
6	Cropland	173.82	40.40	139.10	32.33	115.98	26.96	114.74	26.67	**-82.13**
	Total	430.25	100	430.25	100	430.25	100	430.25	100	

The analysis of land use and land cover changes in the study area showed a reduction in bare land and cropland by 35.34 km² and 59.08 km², respectively. Conversely, other land use/land cover categories displayed both growth and variability in their spatial distribution. These changes are depicted in Figure 4.3.

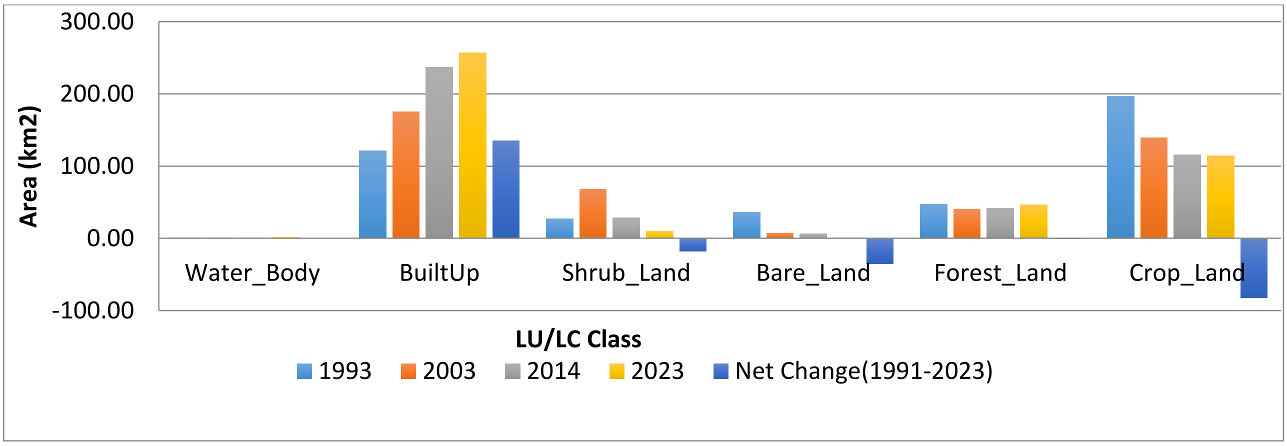

Figure 4.3: LU/LC changes during 1993– 2023 in the study area.

4.3. Land use and land cover change detection

The approach of detecting changes through post-classification comparison showed that different land use and land cover (LULC) classes in the study area underwent changes over the observed period. The conversion matrix tables, analyzed with ArcGIS Pro, depict the relative shifts for each LULC class from 1993 to 2023. Over the past thirty years up to 2023, the land use and land cover (LULC) patterns in the study area have undergone significant changes, as evidenced by shifts in the area covered by various LULC categories. During this period, both bare land and cropland showed a consistent decline, while forest land, shrub land, and water bodies experienced varying changes.

In contrast, built-up areas increased steadily. From the beginning to the end of the period, 22.48 km² of bare land was converted to built-up areas, 10.15 km² to cropland, 1.48 km² to forest land, 1.74 km² to shrub land, and 0.06 km² to water bodies, with only 0.09 km² of bare land remaining unchanged. Additionally, 0.01 km² of built-up area was converted back to bare land, and 17.18 km² was transformed into cropland. Moreover, 4.81 km² of land has been converted to forest, 0.65 km² to shrub land, and 0.41 km² to water bodies. The remaining 121.54 km² of built-up area has not changed.

In terms of cropland, 0.52 km² has been converted to bare land, 90.14 km² to built-up areas, 13.12 km² to forest, 5.01 km² to shrub land, and 1.07 km² to water bodies. The remaining 87.00 km² of cropland remains unchanged. From forestland, 10.27 km² has been changed to built-up areas, 8.46 km² to cropland, 0.61 km² to shrub land, and 0.09 km² to water bodies. The remaining 27.75 km² of forestland remains the same.

Regarding shrub land, 0.05 km² has been converted to bare land, 12.30 km² to built-up areas, 8.78 km² to cropland, 3.93 km² to forest land, and 0.02 km² to water bodies. The remaining 2.28 km² of shrub land remains unchanged.

The water body did not convert into bare land, but 0.38 km² changed into built-up areas. Cropland increased by 0.33 km², while forest land stayed the same at 0.26 km². Additionally, 0.01 km² turned into shrub land, with the remaining 0.28 km² still classified as water body. Detailed statistics from the post-classification analysis and the land use/land cover change map for this period are shown in Table 4.3 and Figure 4.4.

Table 4.3. Post-classification analysis of the study area from (1993-2023).

		Final_Year_2023						
	Class Name	**Bare Land** Area (Km2)	**built-up** Area (Km2)	**Cropland** Area (Km2)	**Forestland** Area (Km2)	**Shrub Land** Area (Km2)	**Water Body** Area (Km2)	**Class Total**
Intial_Year_1993	Bare Land	0.09 0.26%	22.48 62.43%	10.15 28.20%	1.48 4.12%	1.74 4.83%	0.06 0.17%	**36.01**
	built-up	0.00 0.00%	121.54 100.00%	0.00 0.00%	0.00 0.00%	0.00 0.00%	0.00 0.00%	**121.54**
	Cropland	0.52 0.26%	90.14 46.79%	87.00 44.19%	13.12 6.67%	5.01 2.55%	1.07 0.54%	**196.87**
	Forestland	0.00 0.00%	10.27 21.76%	8.46 17.94%	27.75 58.81%	0.61 1.28%	0.09 0.20%	**47.19**
	Shrub Land	0.05 0.18%	12.30 44.92%	8.78 32.10%	3.93 14.38%	2.28 8.34%	0.02 0.08%	**27.37**
	Water Body	0.00 0.00%	0.38 30.22%	0.33 26.44%	0.26 20.34%	0.01 0.94%	0.28 22.06%	**1.26**
	Class Total	**0.67**	**257.12**	**114.74**	**46.55**	**9.65**	**1.53**	**430.25**

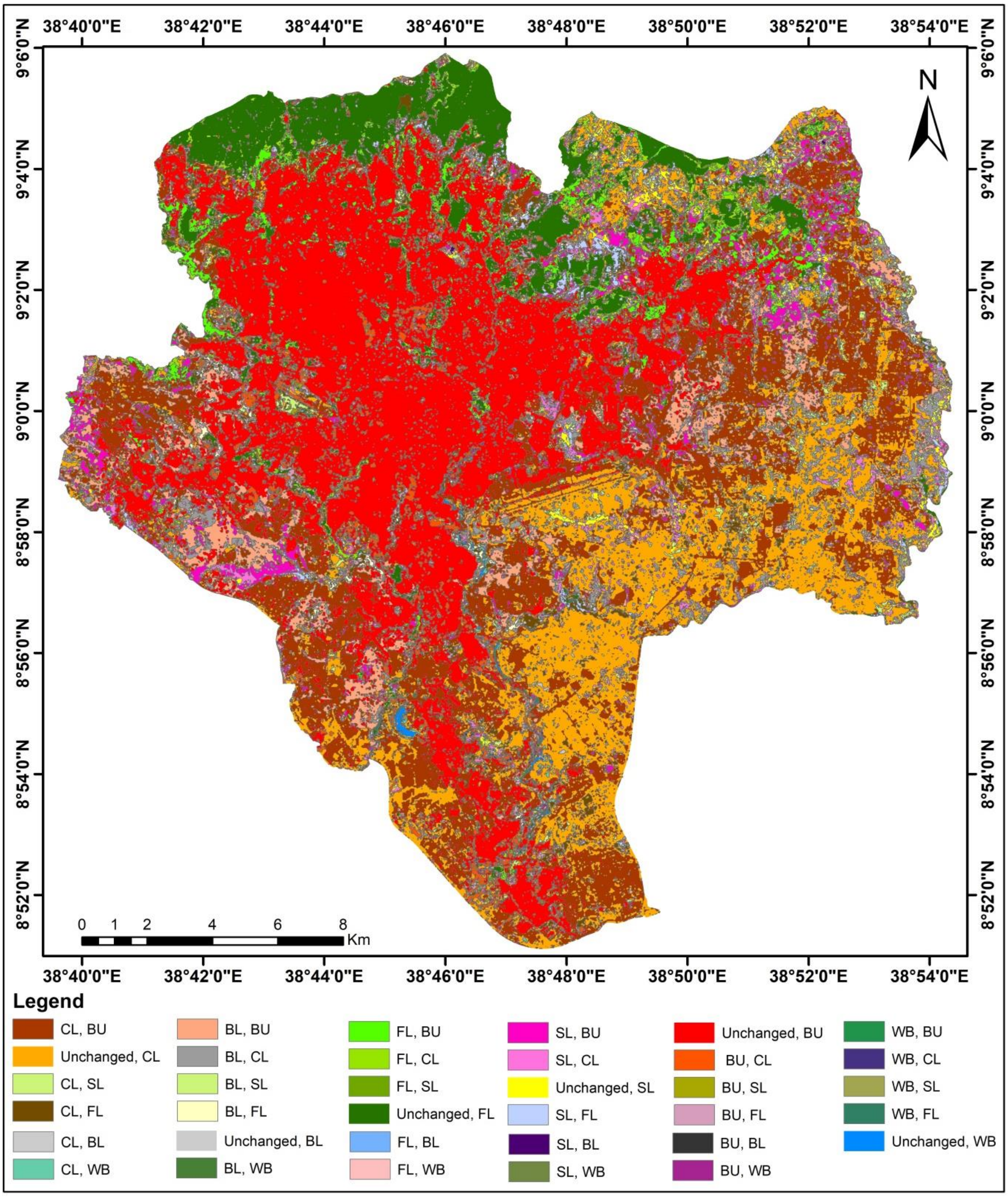

Figure4.4: Land use Land Cover Map of study Area from 1993-2023.

4.4. Accuracy assessment

The assessment of land use/land cover (LU/LC) accuracy for the years 1993, 2003, 2014, and 2023 revealed overall classification accuracies of 88.00%, 90.00%, 91.67%, and 90.00%, respectively. The Kappa statistic for 1993 was 0.86, while for the subsequent years; it was 0.88 in 2003, 0.90 in 2014, and 0.88 in 2023. Detailed information on producer and user accuracy is available in Table 4.4.

Table 4.4: Accuracy assessment statistics for the years 1993, 2003, 2014, and 2023.

	1993		2003		2014		2023	
class Name	producers accuracy	users accuracy	producers accuracy	users accuracy	producers accuracy	users accuracy	producers accuracy	users accuracy
Waterbody	82.00	90.00	88.89	80.00	100.00	100.00	90.00	90.00
Shrub Land	90.00	90.00	90.00	90.00	81.21	90.00	90.00	90.00
Bare Land	89.00	80.00	100.00	90.00	90.00	90.00	76.92	100.00
Forestland	90.00	90.00	75.00	90.00	88.89	80.00	100.00	80.00
Cropland	100.00	90.00	91.00	100.00	100.00	90.00	100.00	90.00
Built-up	82.00	90.00	100.00	90.00	90.91	100.00	90.00	90.00
Overall accuracy	88.00%		90.00%		91.67%		90.00%	
Kappa	0.86		0.88		0.9		0.88	

4.5. Normalized Difference Vegetation Index

This study observed that vegetation cover was at its highest in 1993 and 2003, with peak NDVI values of 0.703 and 0.653, indicating strong vegetation health. There was a decrease in vegetation cover in 2013, with the NDVI dropping to 0.559, but it partially recovered in 2023, reaching 0.629. The northern regions consistently had higher NDVI values, and Entoto Park had the highest NDVI throughout the study. In contrast, built-up areas, water bodies, and the eastern region generally had lower NDVI values. Over time, there has been a gradual decline in vegetation cover, although a slight improvement was noted in 2023 due to the Green Legacy initiative. Figure 4.5 provides detailed findings for 1993, 2003, 2014, and 2023.

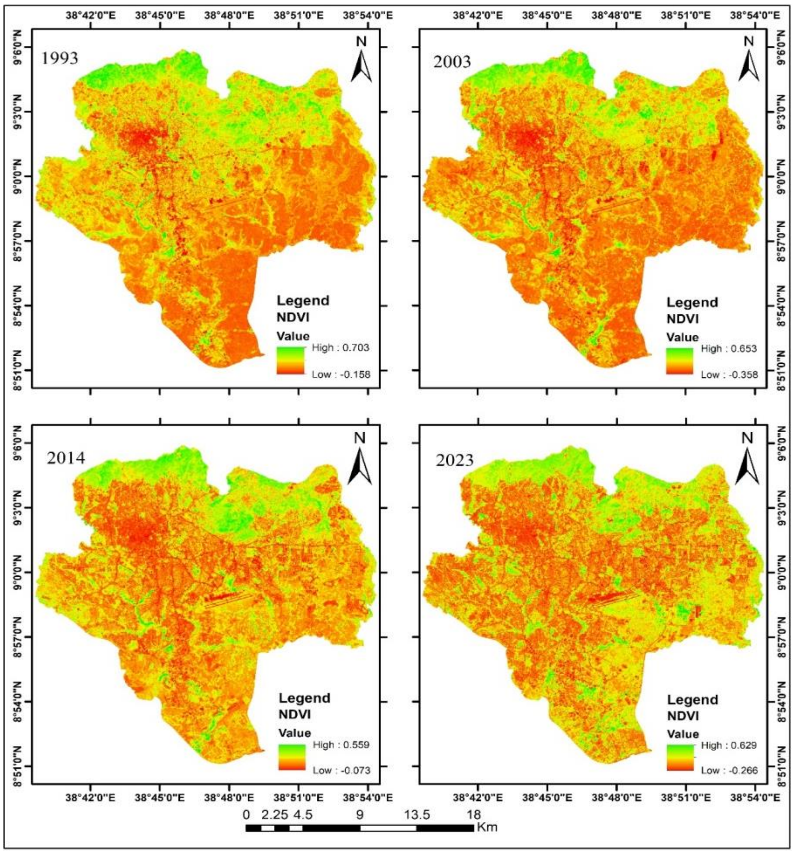

Figure 4.5: Maps of NDVI for the study area in the years 1993, 2003, 2014, and 2023.

4.5.1. Extracted Urban Green Space

In 2023, Gulele and Yeka have the highest green space coverage at 46.05% and 36.33%, respectively. Lemi Kura has 17.82% green space. Akaki-Kality, Lideta, Kolfe, and Bole have green space coverage of 15.81%, 14.15%, 13.20%, and 11.98%, respectively. The inner city areas, Kirkose, Arada, and Addis-Ketema, have lower green space percentages, at 5.39%, 7.88%, and 9.05%, respectively. The details of these findings are shown in Figures 4.6 and 4.7.

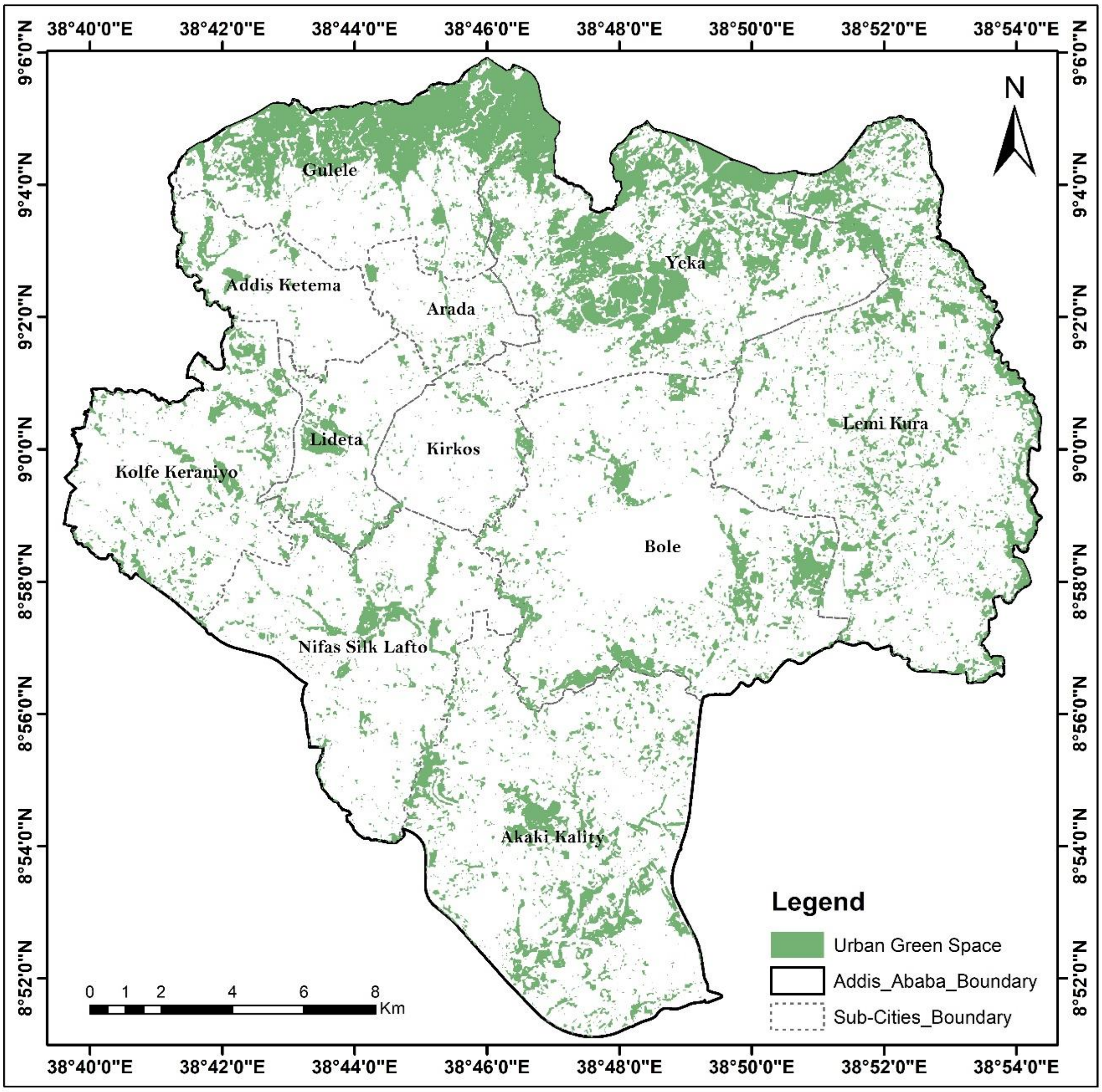

Figure 4.6 Distribution of urban green space map of Study area 2023.

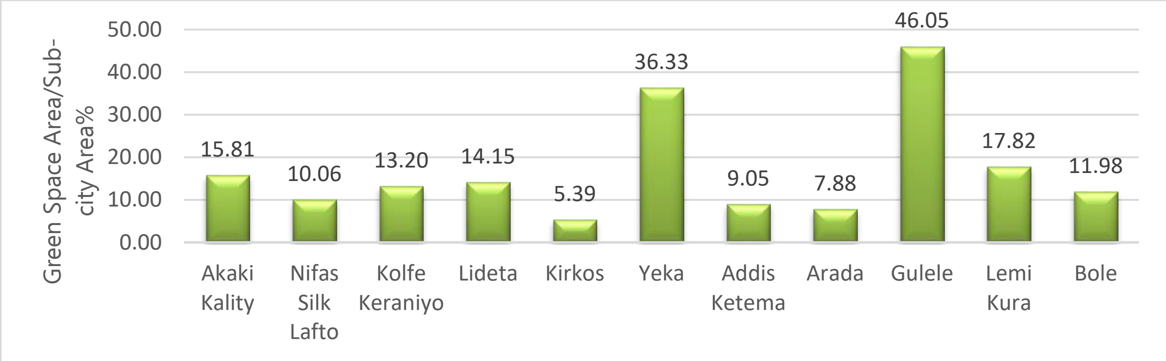

Figure 4.7 Comparison of urban green space in the sub cities of Addis Ababa.

4.6. Population Density

The population density in Addis Ababa varies significantly across its eleven sub-cities. The central areas, which are smaller in size, are the most densely populated. Arada sub-city has the highest density at over 30,683 people per km², making it the most crowded district. Addis Ketema and Kirkos follow with densities of 23,640 and 21,589 people per km², respectively. In contrast, Akaki-Kality, Yeka, Lemi Kura, Gulele, and Bole sub-cities are much less densely populated, with densities below 10,500 people per km². The details of these findings are shown in Figures 4.8 and 4.9.

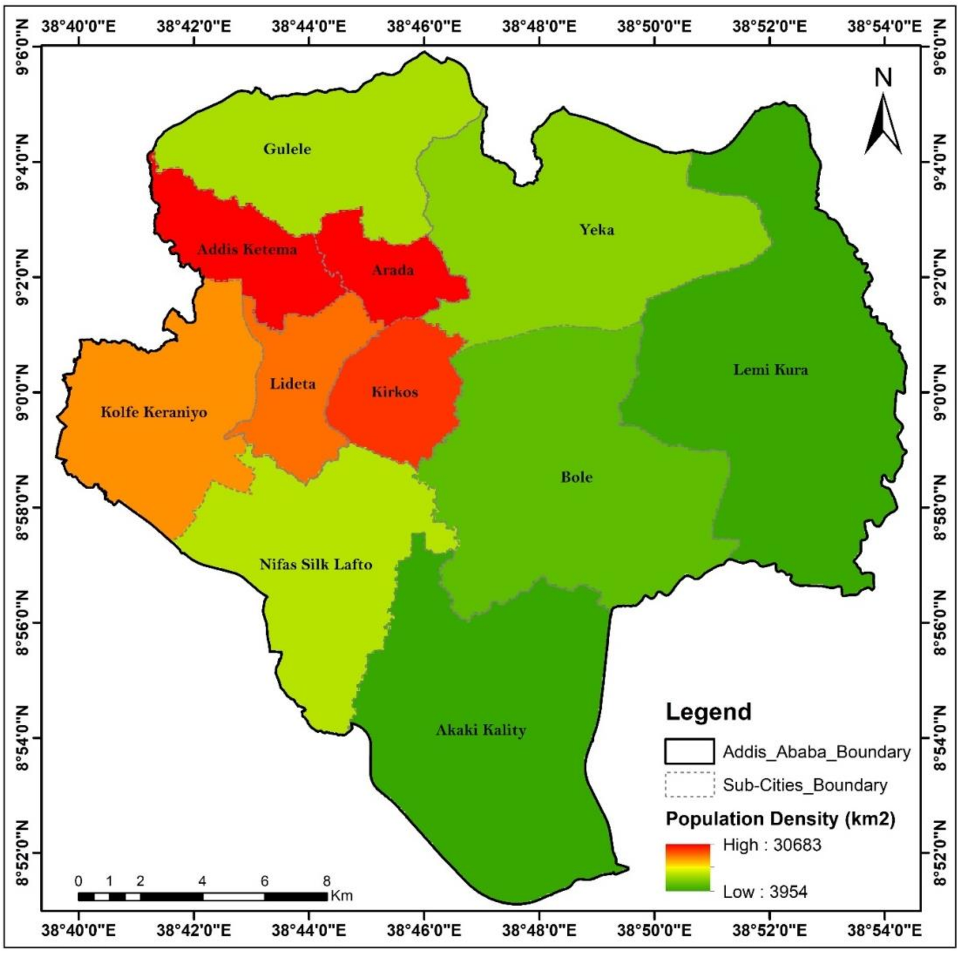

Figure 4.8 Population density distribution map of Addis Ababa sub cities 2023.

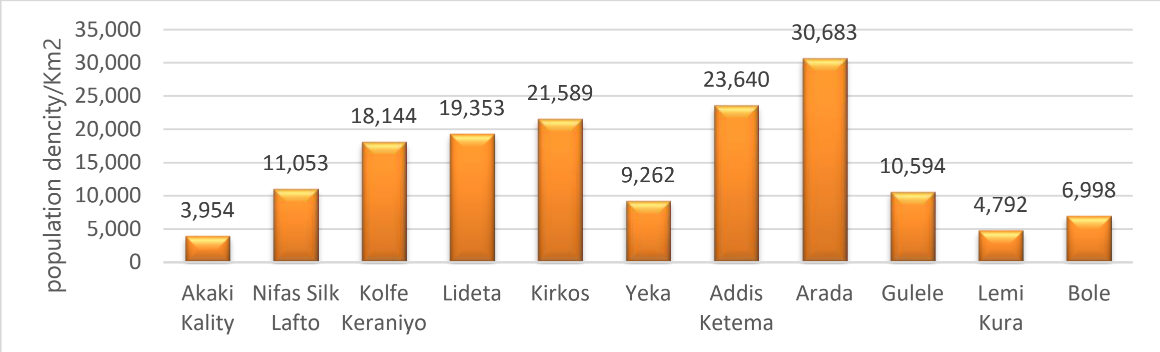

Figure 4.9 Comparison of population density in the sub cities of Addis Ababa.

4.7. Built-up Density

Built-up density in Addis Ababa differs greatly between sub-cities. Central areas are the most densely developed, with Addis Ketema having the highest density at over 68.75%. Other central sub-cities like Arada, Nifas Silk Lafto, Kirkos, Kolfe, and Lideta have densities ranging from 40.57% to 51.60%. Conversely, sub-cities such as Akaki-Kality, Yeka, Lemi Kura, Gulele, and Bole are much less densely built, with densities under 30%. Detailed information is available in Figures 4.10 and 4.11.

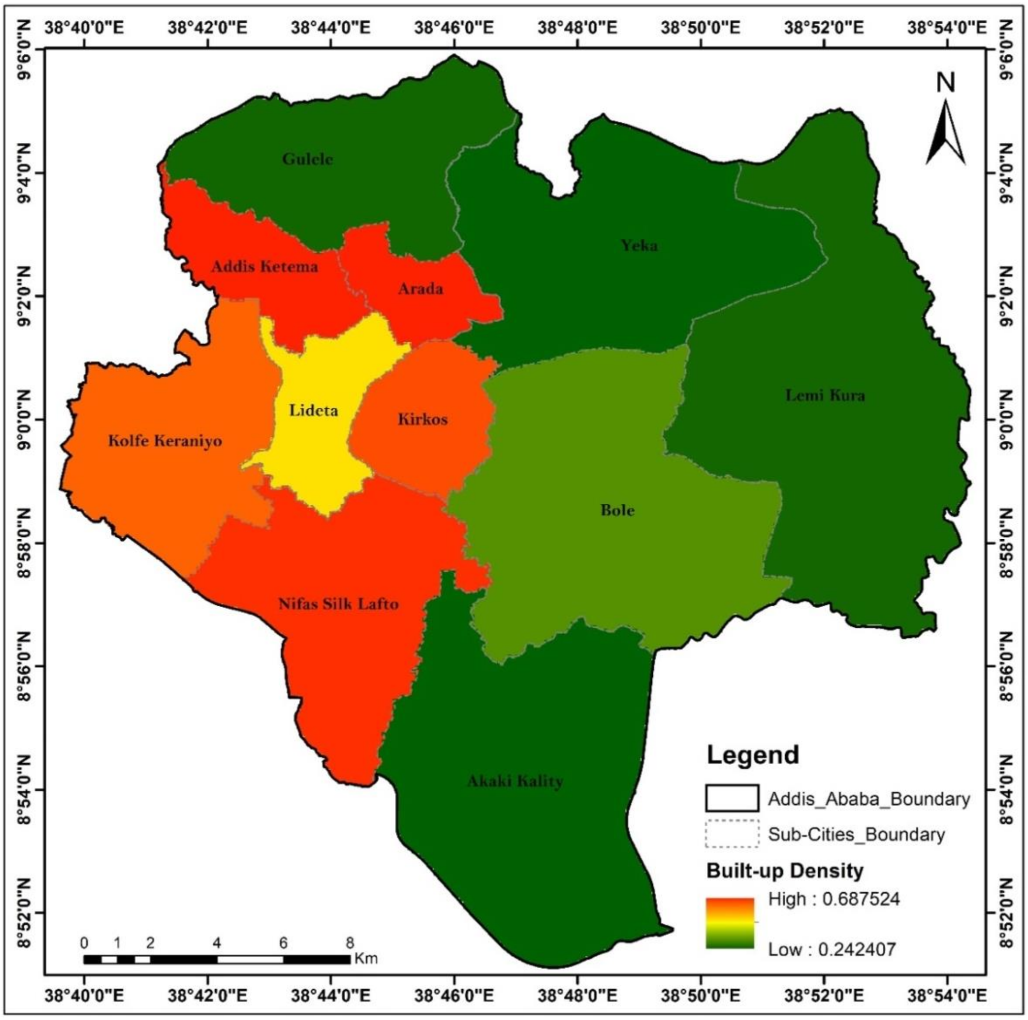

Figure 4.10 Distribution of Built-up Density Map.

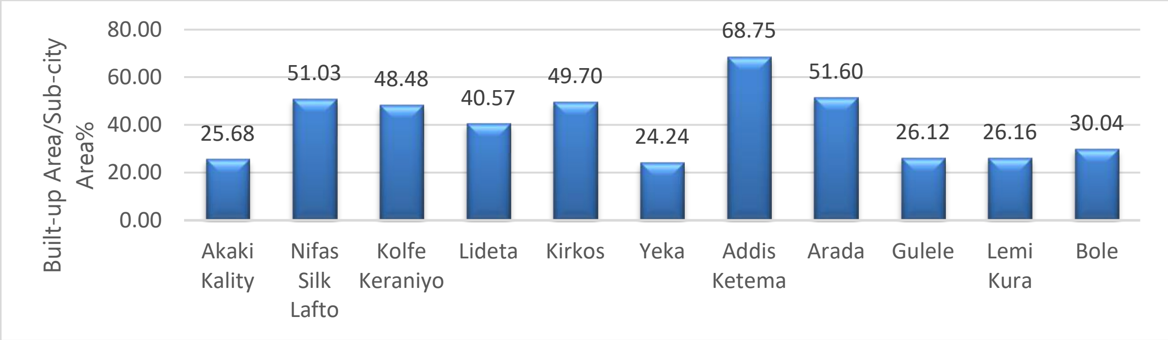

Figure 4.11 Comparison of Building density in the 11 sub city of Addis Ababa.

4.8. Land Surface Temperature

Impervious surfaces like building concrete and asphalt generally show higher surface temperatures compared to vegetated areas. The maximum recorded average surface temperature was 39.17°C, while the minimum was 17.23°C. In terms of zonal mean temperatures, Kirkos, Akaki-Kality, Lideta, Arada, Nifase-Silk Lafto, and Bole sub-cities had an average of 30°C. Addis-Ketema and Kolfe Keraniyo had 29°C, Yeka had 27°C, and Gulele experienced the lowest at 25°C. Detailed information is available in Figures 4.12 and 4.13.

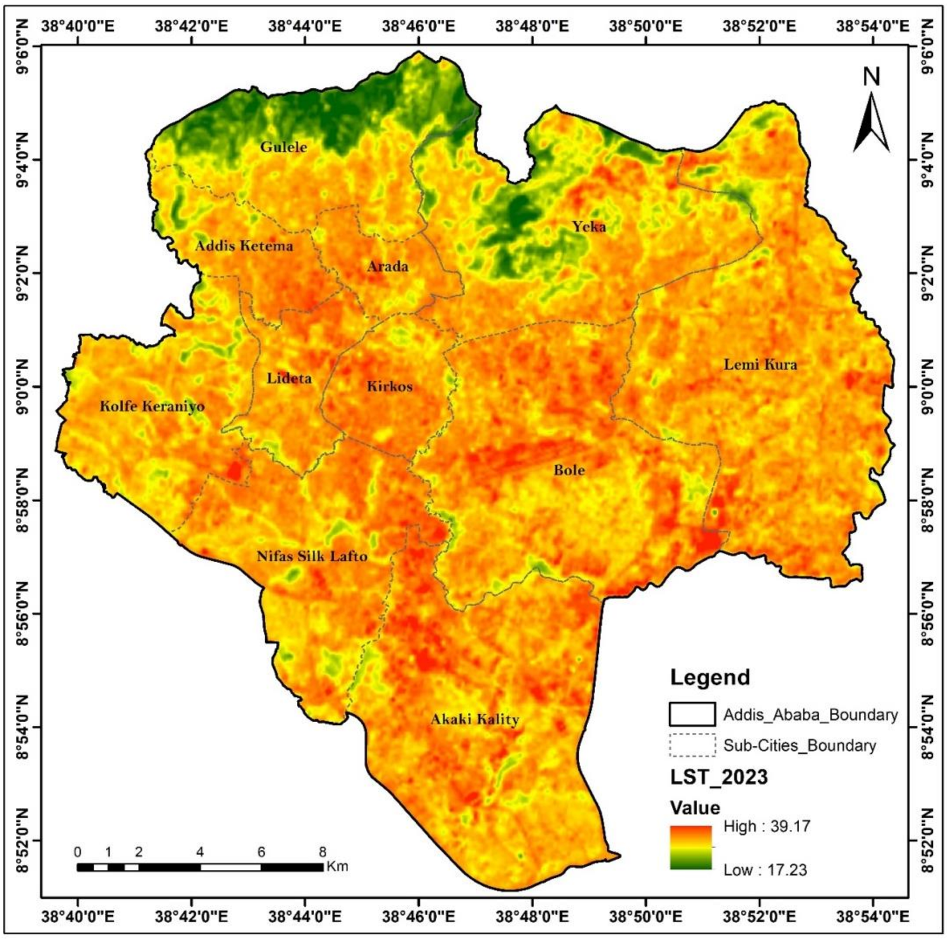

Figure 4.12 Land surface temperature map of the study area.

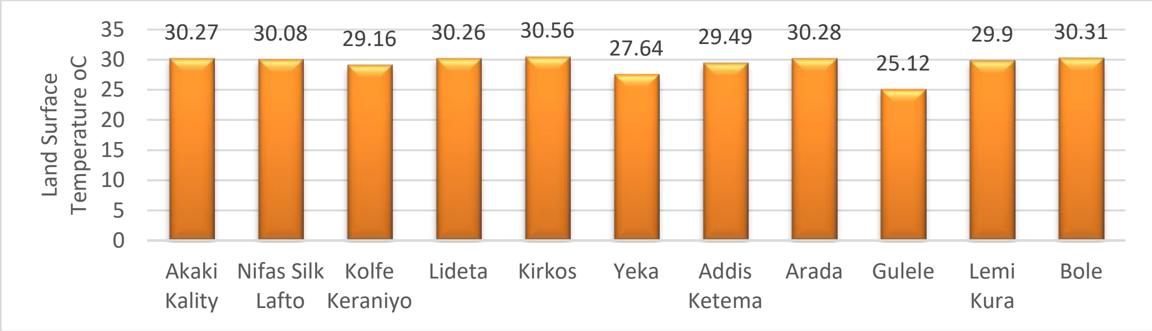

Figure 4.13 Comparison of surface temperature in the sub cities of Addis Ababa.

4.9. Air Quality

The Environmental Protection Authority's 2023 data, shown in Figures 4.14 and 4.15, highlights the concentration of pollutants such as PM2.5, PM10, NO2, SO2, CO, and O3. The highest recorded air quality level was 140.69µg/m³, while the lowest was 62.18µg/m³. The most polluted area was Arada sub-city with 140.69µg/m³. Other highly polluted zones include Kirkos, Bole, Addis-Ketema, and Lideta, with levels between 101-119 µg/m³. Nifas Silk Lafto and Lemi Kura followed, recording 99-100 µg/m³. Kolfe-Keranio and Akaki Kaliti had levels of 90 µg/m³, and Bole, Gulele, and Yeka ranged from 62-83 µg/m³, making them critical areas.

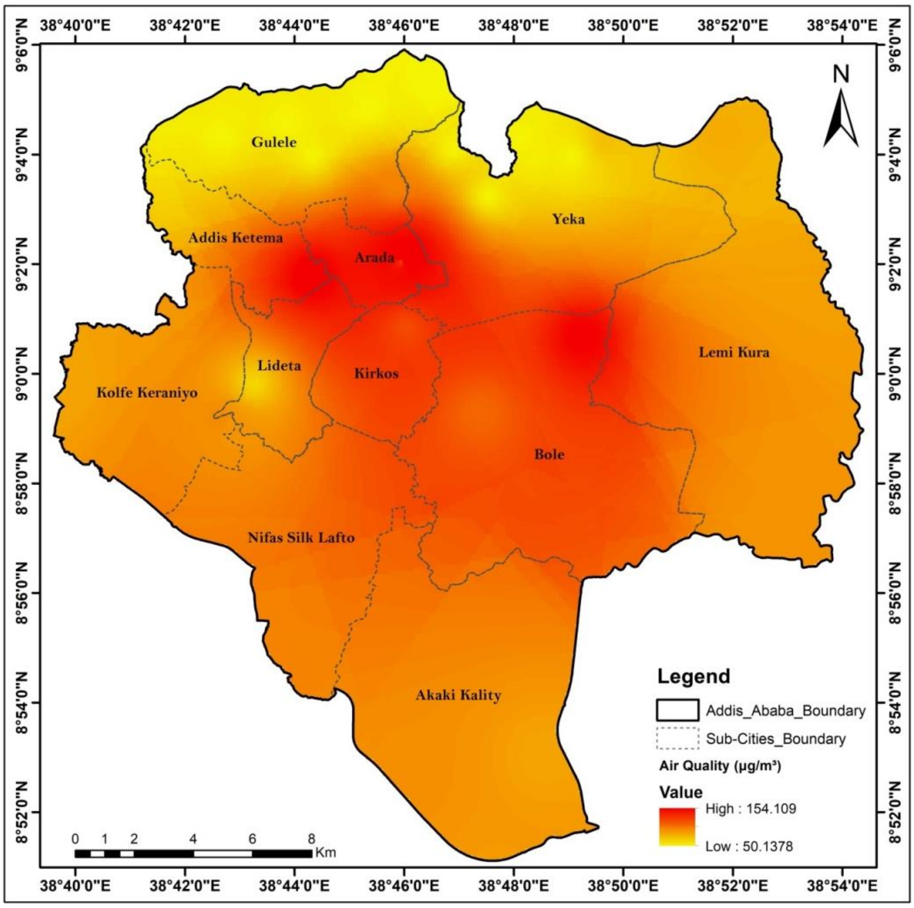

Figure 4.14 Distribution of Green House Gas Emission Map.

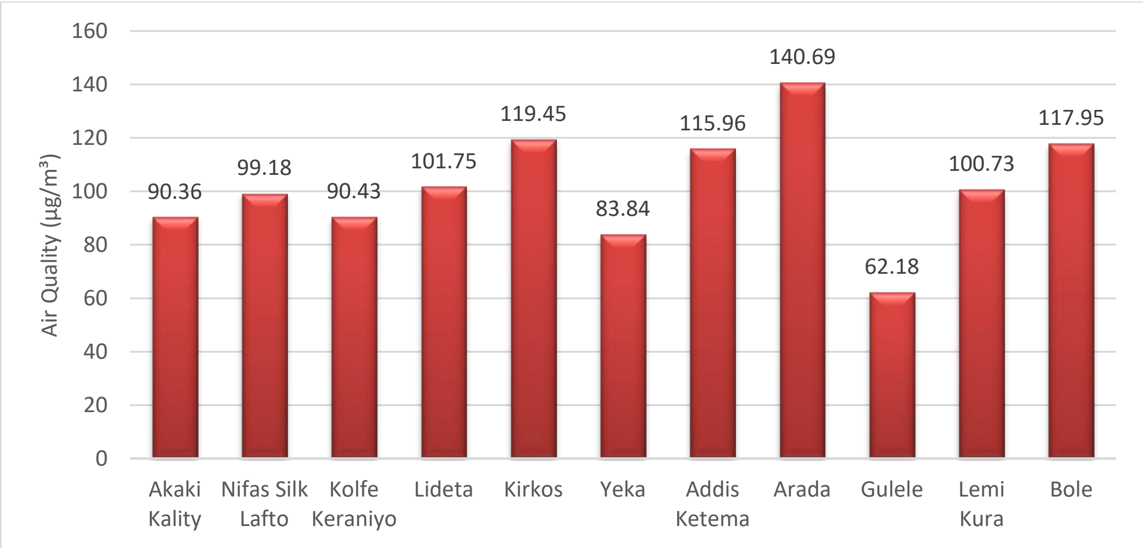

Figure 4.15 Comparison of Air Quality map of in the 11 sub cities of Addis Ababa.

4.10. Overlay Result

Assessing environmental quality is a multidisciplinary and multifaceted task. Overlay analysis provides a direction for what we can expect from a more comprehensive approach. Based on the results of the weighted overlay analysis, there is a need for a universal integration of five key parameters—land-use/land-cover, population density, surface temperature, Air Quality and built-up density—based on the weighting values in Equation 3.9 and Table 3.10. These factors help identify environmental deterioration hotspots, and the generated risk map (Figure 4.16) classifies areas into very high risk, high risk, moderate risk, low risk, and very low risk categories. According to this classification, Addis Ketema falls between very high and high risk, with some areas in the moderate risk category. Arada and Kirkos are classified as high and moderate risk, while Bole, Lideta, Kolfe, Nifas Silk Lafto, and Lemi Kura subcities are within the moderate and low risk categories. Gulele and Yeka subcities are categorized as low and very low risk.

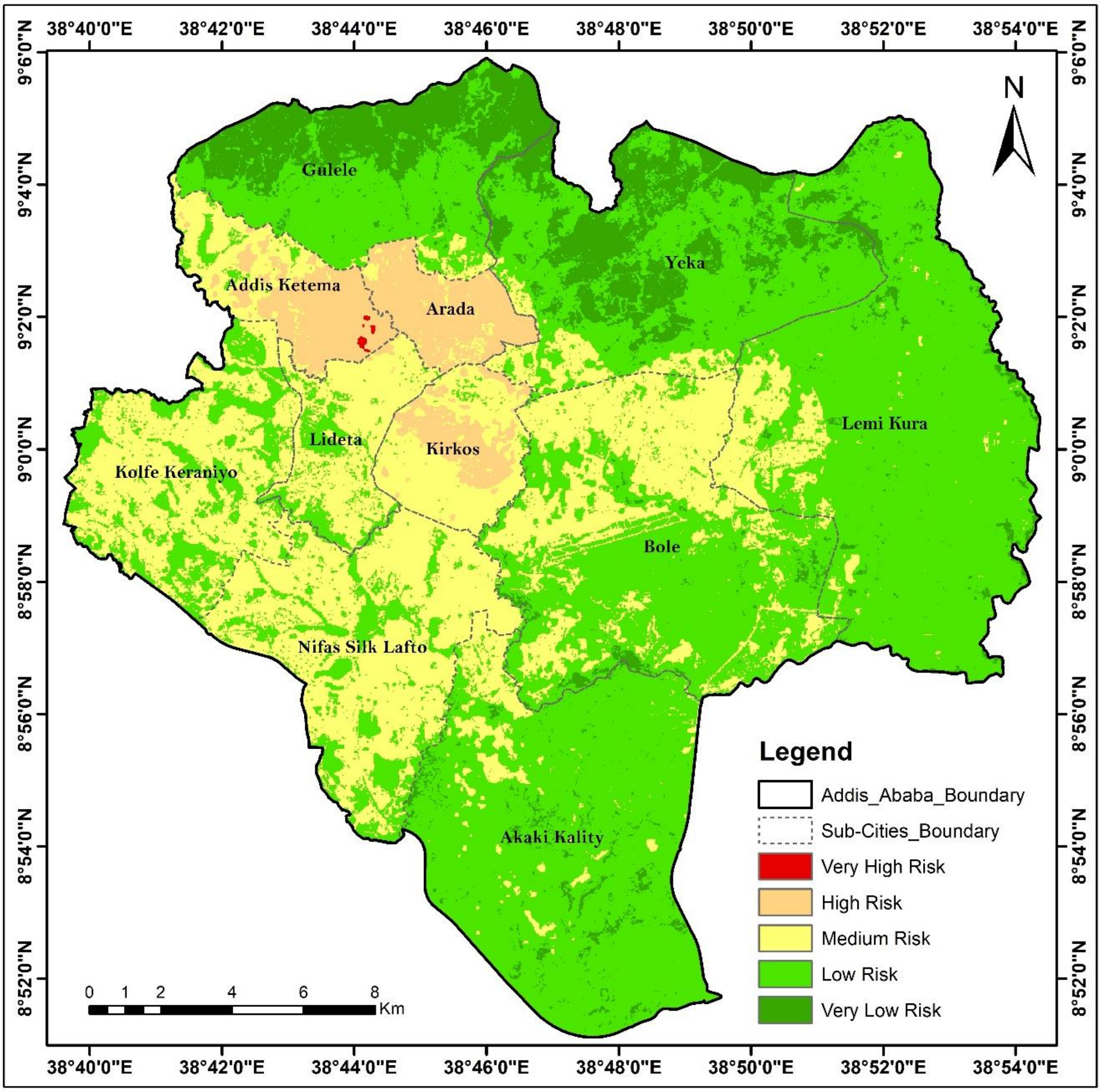

Figure 4.16 Environmental Quality Risk Map of the study area.

Finally, using map algebra and raster calculations, a proportion of the risk map was integrated into the overall urban environmental quality map. Based on the urban environmental quality indicator ratings (Table 3.9), sub-cities with limited green spaces, severe pollution, high heat accumulation, elevated Air Quality, and dense built-up areas were identified as critical regions. In contrast, areas with high vegetation density, low Air Quality, minimal heat islands, low built-up areas, and sparse populations were considered the least environmentally critical (Fig 4.17). According to these results, Addis Ketema Sub-City falls between the very high and high critical categories, while Arada and Kirkos Sub-Cities are in the high to moderate critical range. Lideta, Kolfe, Nifas Silk, Bole, Lemi

Kura, and Akaki Kality are classified as moderate to low critical. Gulele and Yeka Sub-Cities fall within the low to very low critical categories.

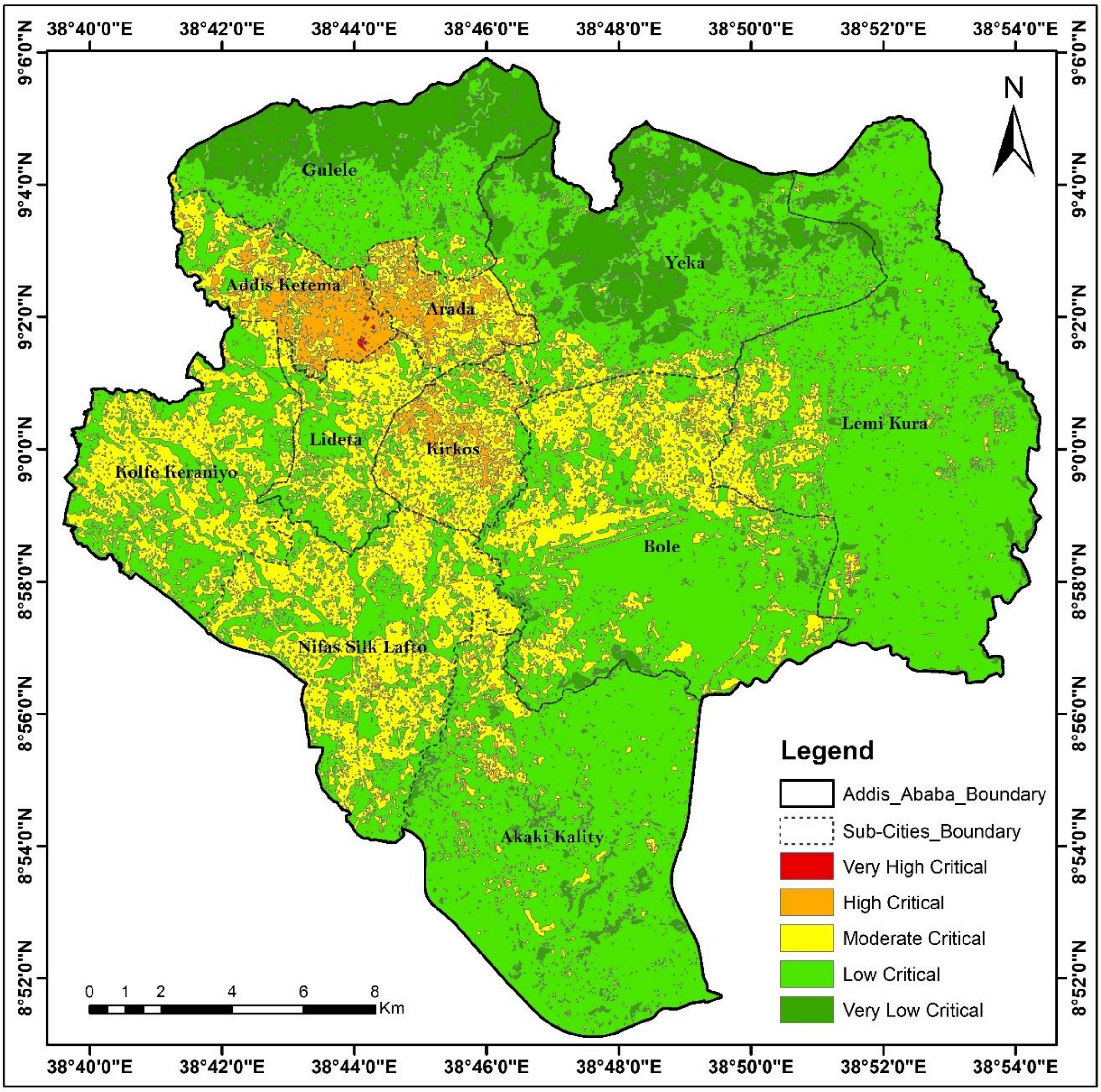

Figure 4.17 Environmental Quality Map of Addis Ababa city.

Table 4.5 Area and level of environmental quality Risk Map and Environmental Quality Map

sub-city	Environmental Quality Risk Map			Environmental Quality Map		
	Area in (km2)	Area in (%)	Risk level	Area in (km2)	Area in (%)	Risk level
Addis Ketema	0.13	0.83	Very High Risk	0.67	4.31	Very High Critical
	8.03	51.86	High Risk	1.66	10.69	High Critical
	6.30	40.69	Medium Risk	6.01	38.70	Moderate Critical
	1.02	6.62	Low Risk	3.35	21.58	Low Critical
	0.00	0.00	Very Low Risk	3.84	24.71	Very Low Critical
Akaki Kality	0.00	0	Very High Risk	1.06	1.60	Very High Critical
	0.00	0	High Risk	1.17	1.78	High Critical
	5.44	8.25	Medium Risk	8.32	12.62	Moderate Critical

	57.93	87.97	Low Risk	14.54	22.06	Low Critical
	2.49	3.77	Very Low Risk	40.84	61.94	Very Low Critical
Arada	0.00	0	Very High Risk	0.24	2.40	Very High Critical
	9.11	91.79	High Risk	0.61	6.11	High Critical
	0.81	8.14	Medium Risk	2.85	28.75	Moderate Critical
	0.01	0.07	Low Risk	2.89	29.07	Low Critical
	0.00	0	Very Low Risk	3.34	33.67	Very Low Critical
Bole	0.00	0	Very High Risk	1.40	2.20	Very High Critical
	0.01	0.01	High Risk	2.22	3.49	High Critical
	26.04	40.96	Medium Risk	13.03	20.50	Moderate Critical
	36.20	56.95	Low Risk	13.72	21.58	Low Critical
	1.32	2.08	Very Low Risk	33.21	52.23	Very Low Critical
Gulele	0.00	0.00	Very High Risk	0.15	0.42	Very High Critical
	0.03	0.10	High Risk	0.56	1.55	High Critical
	1.11	3.07	Medium Risk	4.70	12.92	Moderate Critical
	18.85	51.93	Low Risk	5.84	16.06	Low Critical
	16.30	44.91	Very Low Risk	25.09	69.05	Very Low Critical
Kirkos	0.00	0.00	Very High Risk	0.42	2.86	Very High Critical
	4.77	32.32	High Risk	0.73	4.92	High Critical
	9.70	65.73	Medium Risk	4.49	30.43	Moderate Critical
	0.29	1.95	Low Risk	4.93	33.41	Low Critical
	0.00	0.00	Very Low Risk	4.19	28.38	Very Low Critical
Kolfe Keraniyo	22.53	66.56	Medium Risk	9.17	27.01	Moderate Critical
	11.32	33.44	Low Risk	9.48	27.89	Low Critical
	0.00	0.00	Very Low Risk	15.32	45.10	Very Low Critical
Lemi Kura	7.45	9.34	Medium Risk	12.03	15.08	Moderate Critical
	69.13	86.70	Low Risk	16.76	21.00	Low Critical
	3.15	3.96	Very Low Risk	51.02	63.93	Very Low Critical
Lideta	0.21	1.39	High Risk	0.87	5.82	High Critical
	11.31	75.37	Medium Risk	3.75	25.01	Moderate Critical
	3.49	23.24	Low Risk	4.05	26.99	Low Critical
	0.00	0.00	Very Low Risk	6.33	42.19	Very Low Critical
Nifas Silk Lafto	31.46	76.58	Medium Risk	8.10	19.67	Moderate Critical
	9.62	23.42	Low Risk	13.87	33.69	Low Critical
	0.00	0.00	Very Low Risk	19.20	46.64	Very Low Critical
Yeka	0.07	0.12	High Risk	1.27	2.36	High Critical
	4.40	8.16	Medium Risk	5.93	11.00	Moderate Critical
	30.60	56.82	Low Risk	8.92	16.56	Low Critical
	18.80	34.90	Very Low Risk	37.76	70.08	Very Low Critical

This thesis offers an insight into the potential outcomes of a comprehensive study on urban environmental quality in Addis Ababa, based on classified maps that were analyzed for land-use/land-cover and vegetation classes. Extracting greenness by assessing land-use/land-cover serves as a preliminary method for investigating Urban Environmental Quality (Opeyemi and Trina, 2014). Information on green spaces in urban areas is crucial for maintaining environmental quality. Vegetation plays a significant role in filtering air, water, and sunlight, cooling urban heat, recycling pollutants, moderating the local urban climate, and providing recreational spaces. Consequently, the ecological function of vegetation cover in urban parks can filter up to 85% of air pollutants (Bolund and Hunhamma, 1999).

The comparison between the percentage increase in impervious surfaces and the reduction in greenness may indicate deterioration in environmental quality (Liang and Weng, 2011). Six land-use categories forest land, cropland, shrub land, barren land, built-up areas, and water bodies were identified (see Fig. 4.1 and Table 4.4). Each land use class experienced different rates of increase or decrease in size over the period from 1993 to 2023. Forest land, in particular, exhibited fluctuations, with change rates of -0.70 km²/year, 0.12 km²/year, and 0.56km²/year during the periods of 1993−2003, 2003−2014, and 2014−2023, respectively. These changes are attributed to vegetation being used for housing construction and urban expansion.

The cropland area decreased at a rate of 3.47 km² per year from 1993 to 2003, 2.10 km² per year from 2003 to 2014, and 0.14 km² per year from 2014 to 2023. In contrast, water bodies showed fluctuations, with change rates of -0.03 km² per year from 1993 to 2003, 0.00 km² per year from 2003 to 2014, and 0.06 km² per year from 2014 to 2023, primarily due to deforestation, followed by stabilization through soil conservation and reforestation efforts. Shrub land exhibited variability, with change rates of 4.07 km² per year from 1993 to 2003, -3.57 km² per year from 2003 to 2014, and -2.13 km² per year from 2014 to 2023.

The built-up areas experienced the most significant increase, expanding from 144.60 km² in 1993 to 257.12 km² in 2023. The rate of change was 3.05 km²/year from 1993 to 2003, 5.61km²/year from 2003 to 2014, and 2.26 km²/year from 2014 to 2023. This makes it the most dynamic land cover. The primary cause is evident: urbanization and rapid population growth, which continue to expand each year. However, unbalanced and uncontrolled urbanization has led to environmental degradation and a decline in the quality of urban life (Saied et al., 2004).

The area of bare land decreased from an initial estimate of 36.01 km² in 1993 to 0.67 km² in 2023. The rate of change was -2.91 km² per year from 1993 to 2003, -0.06 km² per year from 2003 to 2014, and -0.62 km² per year from 2014 to 2023. This decline is primarily attributed to afforestation initiatives, rehabilitation programs, and soil conservation efforts.

The Normalized Difference Vegetation Index (NDVI) is a formula that considers the amount of infrared light reflected by plants (Simmon, 1980). Live green plants absorb solar radiation, which they utilize as an energy source during photosynthesis. NDVI is linked to vegetation because green leaves reflect about 20% or less of light in the 0.5 to 0.7 micrometer range (green to red) and approximately 60% in the 0.7 to 1.3 micrometer range (near-infrared). These spectral reflectance values are ratios of reflected to incoming radiation within each spectral band, ranging between 0.0 and 1.0. Consequently, NDVI values range from -1.0 to +1.0. Negative NDVI values (approaching -1) indicate deep water, while values near zero (-0.1 to 0.1) generally represent barren areas like rock, sand, or snow. The nature and extent of these changes vary over time and space, influenced by socio-economic and environmental factors, reflecting a range of other contributing elements.

The results for urban green space across various sub-cities show that Gulele has approximately 46.05% green space coverage, while Yeka has 36.33%, and Lemi Kura has 17.82%. Akaki-Kality, Kolfe, Nifas Silk-Lafto, Lideta, and Bole each have between 10-15% green space coverage. The central areas of the city, Addis Ketema and Arada, have lower levels of green space, with Kirkos having the lowest vegetation cover among all the sub-cities.

Arada, Kirkos, Addis Ketema, and Lideta have the least amount of green space among the sub-cities, ranging from 0.78 to 2.12 km^2, making them the poorest in this aspect. Kolfe and Nifas Silk Lafto also possess limited green areas, measuring between 4.14 and 4.49 km^2. In contrast, Bole and Akaki Kaliti exhibit better green space coverage, spanning from 7.61 to 10.43 km^2. The sub-cities of Gulele, Lemi Kura, and Yeka boast the highest green space areas, with 16.75 km^2, 14.23 km^2, and 19.58 km^2 respectively. When compared to the suggested standard of 7 to 12 km^2 of green space for the city (Zoeshtiagh, 1998), these results indicate that approximately half of Addis Ababa's sub-cities have considerable green spaces contributing positively to environmental quality.

The results indicate a decline in forested areas and an increase in urbanization, cropland, and bare land. These changes, coupled with the impending population explosion and rising immigration, have significantly impacted air quality, posing a major threat to the region's environment and natural systems. The raster calculation overlay analysis provides insight into future trends, suggesting the need for more comprehensive work. Based on the weighted overlay raster analysis, it is essential to integrate five key parameters into a risk map to identify environmental degradation hotspots. Housing density emerges as a critical negative predictor of green space and tree cover (Davies et al., 2008).

Based on the environmental quality results, areas with fewer green spaces, excessive pollution, high heat accumulation, high greenhouse gas emissions, and overcrowding were identified as critical regions. Conversely, areas with high vegetation density, low greenhouse gas emissions, low heat island effects, and sparse populations were deemed environmentally suitable (Fig 4.17). Addis Ketema falls between the categories of very high and high critical areas. Kirkos and Arada sub-cities are within the high and moderate critical categories, while Kolfe, Lideta, Nifas Silk, and Bole are moderate to low critical areas. Gulele, Yeka, Lemi Kura, and Akaki Kaliti are classified as low to very low critical areas. Therefore, the RS and GIS-based methodology described in this study proves useful for assessing environmental quality. Weighted overlay methodologies can also be customized for this purpose, as subject reclassification and map algebra techniques enhance the capabilities of spatial analysis.

The study's accuracy can be improved by utilizing high-resolution satellite imagery. This imagery also allows for more precise change detection analysis. As a result, high-resolution imagery is planned for future studies. Beyond urban environmental quality, the integration of remote sensing (RS) and geographic information systems (GIS) can also be used to assess other critical factors related to ecological and environmental impact, such as air, water, and noise pollution. Additionally, environmental risk and quality maps serve as valuable data sources for city and regional planners.

CHAPTER V: CONCLUSION AND RECOMMENDATION

5.1. Conclusion

Employing a geospatial approach that integrates natural and census data with GIS and remote sensing is highly suitable for tracking changes in urban environmental quality and advancing sustainable environmental planning. Given the limited efforts in the past to assess urban environmental quality, GIS technology is well-suited for storing, manipulating, and mapping urban data, serving as a powerful tool for sustainable environmental quality analysis and planning. The use of integrated data analysis, including remotely sensed satellite imagery and GIS modeling, enables the assessment of the spatial distribution of environmental changes, such as land-use/land-cover classification shifts, NDVI, greenhouse gas emissions, thermal mapping, and demographic challenges in Addis Ababa. Urban Environmental Quality maps derived from these analyses also provide valuable data layers for city planners. Urban Environmental Quality (UEQ) maps serve as valuable data layers for city planners. Based on their overall accuracy, these maps provide a reliable representation of the actual situation. The findings from this study have the potential to influence policy assessment tools and support local governments and environmental agencies in monitoring UEQ. The models developed in this research can assist urban planners not only in assessing the current UEQ condition of a city but also in formulating effective development policies aimed at enhancing future UEQ on a national scale. As a result, land-use planners and policymakers can make informed adjustments to promote sustainable urban landscapes and economic development, contributing to the creation of a greener, more prosperous city with an improved UEQ, rather than one characterized by overcrowding and poor environmental quality. This contributes to significant progress toward achieving greater urban sustainability by prioritizing the long-term integration of environmental protection and social well-being. It suggests that a more sustainable city is characterized by green spaces, which align closely with the key factors determining a city's Urban Environmental Quality (UEQ). Evidently, cities with favorable UEQ conditions have the potential to deliver a more sustainable future.

5.2. Recommendation

The results of this study demonstrate that geospatial approaches and GIS-based multi-criteria analysis (MCA) are essential tools for examining land use and land cover (LULC) changes, as well as for assessing urban green spaces and environmental quality.

- The Environmental Protection Authority and relevant organizations continue to implement and strengthen the Green Legacy Initiative to further enhance urban green spaces and improve the city's environmental quality.
- Urban planners design and implement renewal initiatives and Local Development Programs (LDPs) to effectively address issues like habitat loss and the reduction of green spaces.
- Attention should be given to incorporate additional environmental parameters, such as water and soil, to enhance the accuracy of the results.

REFERENCES

Akanbi, A. Kumar, S. and Fidelis, U. (2013).Application of remote sensing, GIS and GPS for efficient urban management plan – A case study of part of Hyderabad city. Novus International Journal of Engineering & Technology.2 :(1−14).

Angel, S., Parent, J., & Civco, D. L. (2011). The Dimensions of Global Urban Expansion: Estimates and Projections for All Countries, 2000–2050. *Progress in Planning*, 75(2), 53-107.

Aravadinou, D. Evmorfoulou, A. (1999). Planted Lofts, an indirect way for the reintroduction of vegetation into the built-in environment, Ktirio Technical Magazine. 102(in Greek)

Asadi, S. S. Padmaja,V.M.and Reddy, A. (2007). Remote Sensing and GIS Techniques for Evaluation of Groundwater Quality in Municipal Corporation of Hyderabad (Zone-V), India. International Journal of Environmental Research Public Health. 4 :(45-52).

Atlas of Addis Ababa. (2013).

Ayele, A. G., & Tesfaye, B. (2021). Assessing the Impact of Land Use and Land Cover Change on Soil Erosion in Ethiopia Using GIS and Remote Sensing Techniques. Journal of Environmental Management, 286, 112181.

Bolund, P., & Hunhammar, S. (1999). Ecosystem services in urban areas. Ecological Economics, 29(2), 293-301.

Buckley, D.J (1997) .The GIS primer -An introduction to geographic information system.

Campbell, J.B. (1987). Introduction to remote sensing. New York: The Guilford Press.

CBD (Convention on Biological Diversity). (2020). Global Biodiversity Outlook 5. https://www.cbd.int/gbo5

Chiesura, A. (2004). The role of urban parks for the sustainable city. Landscape and Urban Planning, 68(1), 129-138.

Christian, E. and Ugoyibo, O. (2013). Mapping Enugu city’s urban heat Island. International Journal of Environmental Protection and Policy.1: (50−58).

Cohen, B. (2006). Urbanization in Developing Countries: Current Trends, Future Projections, and Key Challenges for Sustainability. *Technology in Society*, 28(1-2), 63-80.

Cromley, E. (2013). Geospatial method in health geographic research. Department of physical Geography and Quaternary Geology Stockholm University Stockholm Sweden.

CSA, (2015) .Central Statistical Agency of Ethiopia

Davies, M., Steadman, P. and Oreszczyn, T. (2008).Strategies for the modification of the urban climate and the consequent impact on building energy use. Energy Policy 36, 45(48–51).

Environmental Protection Agency (EPA): Provides comprehensive data and resources on air quality and AQI measurements.

EPA (U.S. Environmental Protection Agency). (2014). Reducing Urban Heat Islands: Compendium of Strategies.

Esri. (2013) .International user conference. San Diego, California.

European Environment Agency (EEA): Monitors and reports on air quality across Europe, providing detailed data and assessments.

Faber Taylor, A., & Kuo, F. E. (2009). Children with Attention Problems Concentrate Better After Walk in the Park. Journal of Attention Disorders, 12(5), 402-409.

FAO, (2014).Food and Agriculture Organization

Faryadi, Sh. and Taheri, Sh. (2008) Interconnections of Urban Green Spaces and Environmental Quality of Tehran. International Journal Environmental. Research. 3 :(119−210).

Floyd, M. F. (2010). Urban Green Space. In: A. C. C. C. M. (Ed.), The Oxford Handbook of Urban Planning (pp. 451-464). Oxford University Press.

Gencer, E. A. (2013). The Interplay between Urban Development, Vulnerability, and Risk Management: A Conceptual Framework and Its Application to a Case Study of the Istanbul Metropolitan Area. *Natural Hazards*, 69(1), 127-147.

Grimmond, C. S. B. (2007). Urbanization and Global Environmental Change: Local Effects of Urban Warming. *Geographical Journal*, 173(1), 83-88.

Hansen, M. C., Potapov, P. V., Moore, R., Hancher, M., & Heumann, B. (2013). High-Resolution Global Maps of 21st-Century Forest Cover Change. Science, 342(6160), 850-853.

Holt, A. H., et al. (2021). Green Space and Mortality: A Systematic Review and Meta-Analysis. Environmental Research Letters, 16(8), 083015.

Huete, A. R., et al. (2002). Overview of the radiometric and biophysical performance of the MODIS vegetation indices. *Remote Sensing of Environment*, 83(1-2), 195-213.

ILIC, (2015).Integrated land information center

Intergovernmental Panel on Climate Change (IPCC). (2014). Climate Change 2014: Impacts, Adaptation, and Vulnerability. *Cambridge University Press*.

Kaplan, R., & Kaplan, S. (1989). The experience of nature: A psychological perspective. Cambridge University Press.

Kumar, L., & Kumar, V. (2020). Geospatial Technologies for Environmental Management and Sustainable Development. In Geospatial Technologies for Land Resources Mapping and Monitoring (pp. 1-22). Springer.

Kuo, F. E. (2003). The Role of Arboriculture in a Healthy Social Ecology. Journal of Arboriculture, 29(3), 148-155.

Kuo, F. E., & Sullivan, W. C. (2001). Environment and crime in the inner city: Does vegetation reduce crime? Environment and Behavior, 33(3), 343-367.

Landsberg, H. E. (1981). The Urban Climate. *International Geophysics Series* (Vol. 28). Academic Press.

Liang, B. and Weng, Q. (2011).Assessing Urban Environmental Quality Change of Indianapolis, United States, by the Remote Sensing and GIS Integration. Ieee Journal of Selected in Applied Earth Observations and Remote Sensing. 4 :(1).

Lillesand, T.M. and Keifer, W. (1994). Remote sensing and image interpretation. New York: Wiley.

Low, N. Gleeson, B. Green, R. and Radovic, D. (2007). The Green City, Sustainable Homes, Sustainable Suburbs. London: Rutledge. (80-101)

McHarg, I.(1969). Use of the overlay method .Environmental Planning Design with Nature

Miller, J. R. (2005). Biodiversity conservation and the extinction of experience. Trends in Ecology & Evolution, 20(8), 430-434.

NMI. (2015), National Meteorological Institute

Oke, T. R. (1987). Boundary Layer Climates. *Routledge*.

Opeyemi, A. and Trina, W. (2014). Potential application of change in urban green space as an indicator of urban environmental quality change. Universal Journal of Geoscience 2 :(222−228).

Pettorelli, N. (2013). The Normalized Difference Vegetation Index. Oxford University Press.

Rashmin, G. (2004).use of GIS for Environmental Impact Assessment: An interdisciplinary Approach. Interdisciplinary Science Review, 29 :(1), (1-11)

Richard G. Davies, Olga Barbosa, Richard A. Fuller, Jamie Tratalos, Nicholas Burke, Daniel Lewis, Philip H. Warren and Kevin J. Gaston (2008). City-wide relationships between green spaces, urban land use and topography. Urban Ecosystem. 11 :(269–287).

Rouse, J. W., Haas, R. H., Schell, J. A., & Deering, D. W. (1974). Monitoring vegetation systems in the Great Plains with ERTS. *Proceedings of the Third Earth Resources Technology Satellite-1 Symposium*, 1, 309-317.

Saaty, T.L. 1980. The Analytic Hierarchy Process. McGraw-Hill. Saied, P. Ahmad, S. Heshmi, A. & Hussain, J.(2004). Greenery (Green Space) Percentage Estimation Using Band Ratio, NDVI From Landsat Enhanced Thematic Mapper (ETM)-2002 & An Application Of Geographic Information System (GIS) Techniques, Dezful-Andimeshk, Khuzestan South-West Iran.8th International Seminar on Map India, 7-9 February, 2005New Delhi.

Simmon, R. (1980) Normalized Difference Vegetation Index (NDVI) Analysis for Forestry and Crop Managemen (41-48)

Thompson, C. (2002).urban open space in the 21stcentury Landscape and Urban Planning; 60 :(2) (59-72)

Triantaphyllou, E and Mann,S.H.(1995),Using the Analytical Hierarchy process for decision making in engineering .(80-83)

Tsouchlaraki, A. Venieri,D. Dimosand,G. Achilleos,G. (2010). Spatiotemporal and qualitative analysis and evaluation of urban green using a geographic information system. 3rdInternational Conference on Cartography and GIS (35-50)

Tucker, C. J. (1979). Red and photographic infrared linear combinations for monitoring vegetation. *Remote Sensing of Environment*, 8(2), 127-150.

Turner, W., Spector, S., & Oppenheimer, M. (2015). Remote Sensing for Resilience: Improving Human Capacity to Adapt to Environmental Change in Africa. Nature Climate Change, 5(10), 936-940.

Twumasi1,Y. and Merem ,.E (2006).GIS and Remote Sensing Applications in the Assessment of Change within a Coastal Environment in the Niger Delta Region of Nigeria International. Journal of Environmental Research Public Health. 3 :(98−106).

Tzoulas, K., Korpela, K., Venn, S., & Ylen, H. (2007). Promoting ecosystem and human health in urban areas using green infrastructure: A literature review. Landscape and Urban Planning, 81(3), 167-178.

United Nations Department of Economic and Social Affairs (UN DESA). (2019). World Urbanization Prospects: The 2018 Revision. *UN DESA Population Division*.

Valor, E. & Caselles, V. (1996).Mapping land surface emissivity from NDVI. Application to European, African and South-American areas. Remote Sensing of Environment, (57,167-184)

Velarde, M.D Fry, Tveit, M. (2007) .Health effects of viewing landscapes – Landscape types in environmental psychology (101-103)

Weng, Q., & Yang, S. (2006). Urban Air Pollution Patterns, Land Use, and Thermal Landscape: An Examination of the Linkages Using GIS. *Remote Sensing of Environment*, 104(2), 189-203.

WHO. (2016). Urban green spaces and health: A review of evidence. World Health Organization.

Wolch, J. R., Byrne, J., & Newell, J. P. (2014). Urban green space, public health, and environmental justice: The challenge of making cities "just green enough." Landscape and Urban Planning, 125, 234-244.

World Health Organization (WHO): Offers guidelines and reports on air quality and its impact on health.

Zhao, Y., Huang, J., & Xu, S. (2016). Green space in urban areas and its contribution to urban heat island mitigation: A review. Sustainability, 8(4), 386.

Zoeshtiagh, S. (1998). The abstract of Tehran comprehensive plan: conservation and redevelopment planning and architecture of Iran. Tehran: the company of urban processing and planning. (20-31).

APPENDICES

Appendix 1: Accuracy Assessment Sample Points

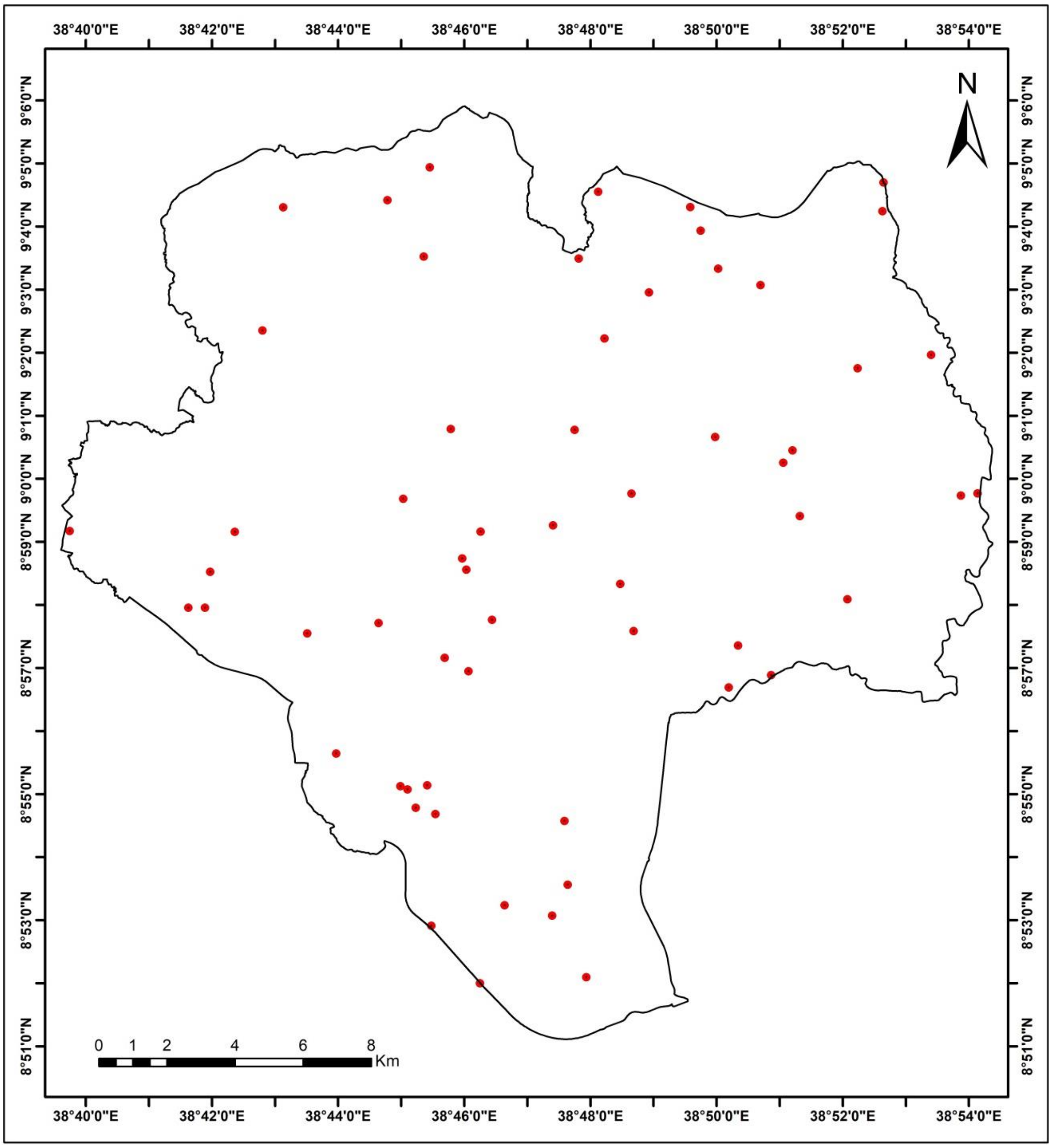

Appendix 2: Pair-wise comparison matrix to calculate weight of factors for environmental quality

Factors	LULC	Air Quality	Population Density	Built-up Density	Surface Temperature	Weight
LULC	1	1	1	1	1 1/2	21.04%
Air Quality	1	1	2	1	1	23.25%
Population Density	1	1/2	1	2	1	20.41%
Built-up Density	1	1	1/2	1	1	17.34%
Surface Temperature	2/3	1	1	1	1	17.95%

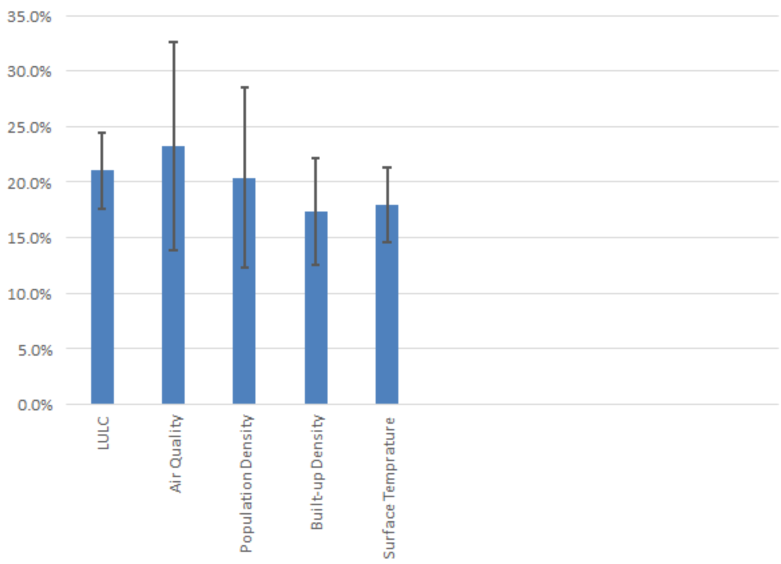

Appendix 3: Assessment of environmental rate of change during 1993-2023

No	Land Cover Type	1993-2003		Rate of change 1993–2003 (km2 /year)	2003-2014		Rate of change 2003–2014 (km2 /year)	2014-2023		Rate of change 2014–2023 (km2 /year)	1993-2023		Rate of change 1993–2023 (km2 /year)
		Area(KM2)	Area(%)		Area(KM2)	Area(%)		Area(KM2)	Area(%)		Area(KM2)	Area(%)	
1	Water_Body	-0.282	-0.066	**-0.028**	0.012	0.003	**0.001**	0.533	0.124	**0.059**	0.263	0.061	**0.009**
2	BuiltUp	30.477	7.084	**3.048**	61.704	14.342	**5.609**	20.343	4.728	**2.260**	112.524	26.153	**3.751**
3	Shrub_Land	40.655	9.449	**4.065**	-39.231	-9.118	**-3.566**	-19.144	-4.449	**-2.127**	-17.720	-4.119	**-0.591**
4	Bare_Land	-29.104	-6.765	**-2.910**	-0.701	-0.163	**-0.064**	-5.539	-1.287	**-0.615**	-35.344	-8.215	**-1.178**
5	Forest_Land	-7.028	-1.634	**-0.703**	1.336	0.310	**0.121**	5.052	1.174	**0.561**	-0.641	-0.149	**-0.021**
6	Crop_Land	-34.716	-8.069	**-3.472**	-23.120	-5.374	**-2.102**	-1.245	-0.289	**-0.138**	-59.081	-13.732	**-1.969**

Appendix 4: Multi regression ordinary list square result.

Summary of OLS Results - Model Variables								
Variable	Coefficient [a]	Std Error	t-Statistic	Probability [b]	Robust_t	Robust_SE	Robust_Pr [b]	VIF [c]
Intercept	0.737560	0.108715	6.784344	0.000213*	0.073985	9.969012	0.000000*	--------
LST	0.010060	0.006986	1.440019	0.193181	0.002069	4.861772	0.001955*	6.020217
air quality	-0.006501	0.001602	-4.057827	0.004954*	0.000930	-6.993452	0.000159*	6.008995
population	-0.000009	0.000003	-3.109865	0.017055*	0.000001	-7.886904	0.000036*	3.101970

OLS Diagnostics			
Input Features:	Addis Ababa sub cities	Dependent Variable:	NDVI
Number of Observations:	11	Akaike's Information Criterion (AICc) [d]:	-27.783352
Multiple R-Squared [d]:	0.964289	Adjusted R-Squared [d]:	0.948984
Joint F-Statistic [e]:	63.005578	Prob(>F), (3,7) degrees of freedom:	0.000020*
Joint Wald Statistic [e]:	477.468413	Prob(>chi-squared), (3) degrees of freedom:	0.000000*
Koenker (BP) Statistic [f]:	6.963602	Prob(>chi-squared), (3) degrees of freedom:	0.073067
Jarque-Bera Statistic [g]:	1.299721	Prob(>chi-squared), (2) degrees of freedom:	0.522119

Notes on Interpretation

* An asterisk next to a number indicates a statistically significant p-value ($p < 0.01$).

[a] Coefficient: Represents the strength and type of relationship between each explanatory variable and the dependent variable.

[b] Probability and Robust Probability (Robust_Pr): Asterisk (*) indicates a coefficient is statistically significant ($p < 0.01$); if the Koenker

(BP) Statistic [f] is statistically significant, use the Robust Probability column (Robust_Pr) to determine coefficient significance.

[c] Variance Inflation Factor (VIF): Large Variance Inflation Factor (VIF) values (> 7.5) indicate redundancy among explanatory variables.

[d] R-Squared and Akaike's Information Criterion (AICc): Measures of model fit/performance.

[e] Joint F and Wald Statistics: Asterisk (*) indicates overall model significance ($p < 0.01$); if the Koenker (BP) Statistic [f] is

Statistically significant, use the Wald Statistic to determine overall model significance.

[f] Koenker (BP) Statistic: When this test is statistically significant ($p < 0.01$), the relationships modeled are not consistent (either due to

Non-stationarity or heteroskedasticity). You should rely on the Robust Probabilities (Robust_Pr) to determine coefficient significance and on the

Wald Statistic to determine overall model significance.

[g] Jarque-Bera Statistic: When this test is statistically significant ($p < 0.01$) model predictions are biased (the residuals are not normally distributed).

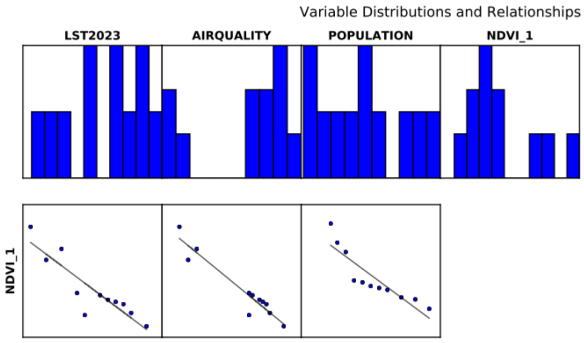

The above graphs are Histograms and Scatterplots for each explanatory variable and the dependent variable. The histograms show how each variable is distributed. OLS does not require variables to be normally distributed. However, if you are having trouble finding a properly-specified model, you can try transforming strongly skewed variables to see if you get a better result.

Each scatterplot depicts the relationship between an explanatory variable and the dependent variable. Strong relationships appear as diagonals and the direction of the slant indicates if the relationship is positive or negative. Try transforming your variables if you detect any non-linear relationships. For more information see the Regression Analysis Basics documentation.

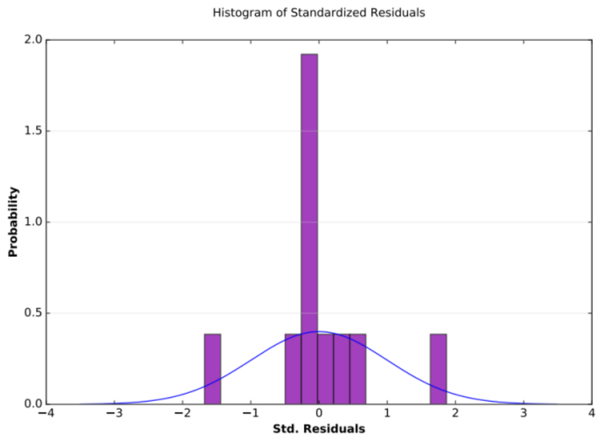

Ideally the histogram of your residuals would match the normal curve, indicated above in blue. If the histogram looks very different from the normal curve, you may have a biased model. If this bias is significant it will also be represented by a statistically significant Jarque-Bera p-value (*).

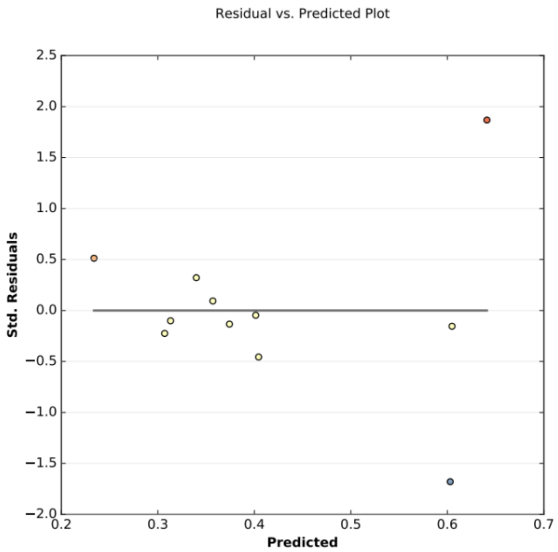

This is a graph of residuals (model over and under predictions) in relation to predicted dependent variable values. For a properly specified model, this scatterplot will have little structure, and look random (see graph on the right). If there is a structure to this plot, the type of structure may be a valuable clue to help you figure out what's going on.

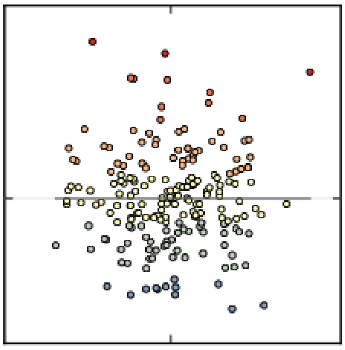

Ordinary Least Squares Parameters

Parameter Name	Input Value
Input Features	Addis Ababa Sub Cities
Unique ID Field	Id
Output Feature Class	None
Dependent Variable	NDVI
Explanatory Variables	LST
	AIRQUALITY
	POPULATION
Selection Set	False